

Copyright
by
Holly C. Mein
2019

THE MAGNETIC MOMENT OF LEPTONS
AT HIGH TEMPERATURES

by

Holly C. Mein, B.S.

THESIS

Presented to the Faculty of
The University of Houston-Clear Lake
In Partial Fulfillment
Of the Requirements
For the Degree

MASTER OF SCIENCE

in Physics

THE UNIVERSITY OF HOUSTON-CLEAR LAKE

MAY, 2019

THE MAGNETIC MOMENT OF LEPTONS
AT HIGH TEMPERATURES

by

Holly C. Mein

APPROVED BY

Samina S. Masood, PhD., Chair

Van E. Mayes, PhD., Committee Member

David Garrison, Ph.D., Committee Member

RECEIVED/APPROVED BY THE COLLEGE OF SCIENCE AND ENGINEERING

Said Bettayeb, Ph.D., Associate Dean

Ju Kim, Ph.D., Interim Dean

Acknowledgements

There are a number of people who have been instrumental to my success in earning my Master's in Physics. The first is my husband, Michael Mein, for always encouraging me to achieve my goals and being my personal cheerleader. His encouragement pushed me forward and was the calm voice of reason in hard times. I could not have done it without his love and support.

Thank you to my parents and sister for always supporting me and making me the driven, passionate person I am today. Their encouragement to follow my dreams made me feel anything is possible with hard work.

Thank you to my committee for being present when I had questions and helping with my thesis. The support I received during my graduate career helped propel me forward through difficult times.

I want to express sincere gratitude to my advisor, Dr. Samina Masood. Her passion for research and dedication to her students is inspiring. Working for Boeing while being a full-time graduate student was difficult, but the flexibility and support I received from Dr. Masood made success possible. I never could have completed my thesis without her guidance and immeasurable help. She made herself available at all times of the day and took as long as necessary to make sure I understood difficult concepts. Dr. Masood is an awe-inspiring role model who shows me daily how being a woman in physics is a strength not a weakness.

ABSTRACT

THE MAGNETIC MOMENT OF LEPTONS AT HIGH TEMPERATURES

Holly C. Mein
University of Houston-Clear Lake, 2019

Thesis Chair: Samina Masood, PhD.

The magnetic moment is a measure of the interaction of charged particles with the magnetic field. It depends on the mass of the particles. All charged particles have an intrinsic magnetic moment due to their intrinsic spin, whereas the neutral particles do not exhibit intrinsic magnetic moment. Charged particles can induce a magnetic moment to neutral particles. This induced magnetic moment of neutral particles is a perturbative effective and is produced radiatively at higher orders of perturbation. There is still information not known about the structure and magnetic moment of particles. The magnetic moment of particles is not precisely calculated for cases when the effective mass of particles is modified due to radiative corrections at high energies. Therefore, the magnetic moment of particles needs to be calculated for individual particles that interact differently. This thesis is comprised of an overview of the magnetic moment of all flavors of leptons in vacuum (at $T=0$) as well as in a medium. Due to the interaction with the medium, the effect of high temperatures of the medium contribute to the magnetic moment. Some of the cosmological applications of temperature dependent magnetic moment are also discussed.

TABLE OF CONTENTS

List of Tables	viii
List of Figures	ix
INTRODUCTION	1
CHAPTER I: MOTIVATION	4
Development of Quantum Field Theory	6
Quantum Electrodynamics	10
Feynman Diagrams in QED	13
Decay Rates and Cross-sections	15
Renormalization of QED	18
Radiative Corrections at Finite Temperature	19
Renormalization in QED in Finite Temperature	21
CHAPTER II: ELECTROMAGNETIC FORM FACTORS	24
Dirac Neutrinos	24
Charge Radius	26
Electric Dipole Moment	27
Anapole Moment	27
Magnetic Dipole Moment of Leptons	28
First Generation Lepton Flavor Electron (e and νe)	28
Second Generation Lepton Flavor Muon (μ and $\nu\mu$)	35
Third Generation Lepton Flavor Tau (τ and $\nu\tau$)	39
CHAPTER III: MAGNETIC MOMENT OF LEPTONS IN HIGH TEMPERATURE ..	44
First Generation Lepton Flavor Electron (e and νe)	45
Electron	45
Electron Neutrino	48
Second Generation Lepton Flavor Muon (μ and $\nu\mu$)	52
Muon	52
Muon Neutrino	53
Third Generation Lepton Flavor Tau (τ and $\nu\tau$)	54
Tau	54
Tau Neutrino	54
Majorana Neutrinos	55
Weyl Massless Neutrino	58
CHAPTER IV: DISCUSSION	61

REFERENCES 75

LIST OF TABLES

Table [1.4.1]: Feynman Diagram Rules.....	14
Table [5.1.1]: Magnetic Moment of Charged Leptons around Nucleosynthesis in the Universe	67
Table [5.1.2.a]: Magnetic Moment of Neutrinos (Upper Bounds)	71
Table [5.1.2.b]: Magnetic Moment of Neutrinos (Lower Bounds).....	71

LIST OF FIGURES

Figure [1.5.1]: Radiative Corrections for Decay of $Z^0 \rightarrow l + l^-$	16
Figure [2.5.1]: Diagram of intrinsic magnetic moment of an electron	29
Figure [2.5.2]: Emission and Absorption of Photons	31
Figure [2.5.3]: The helicity of a particle	32
Figure [2.5.4]: Bubble diagram for electron neutrino in the minimal standard model.....	34
Figure [2.5.5]: Tadpole diagram for electron neutrino in the minimal standard model.....	34
Figure [2.5.6]: Bubble diagram for muon neutrino in the minimal standard model.....	38
Figure [2.5.7]: Tadpole diagram for muon neutrino in the minimal standard model.....	38
Figure [2.5.8]: Bubble diagram for tau neutrino in the minimal standard model.....	42
Figure [2.5.9]: Tadpole diagram for tau neutrino in the minimal standard model.	42
Figure [5.1.1.a]: Electron Magnetic Moment vs Tm^2	65
Figure [5.1.1.b]: Muon Magnetic Moment vs Tm^2	65
Figure [5.1.1.c]: Tau Magnetic Moment vs Tm^2	66
Figure [5.1.2]: Charged Lepton Magnetic Moment vs Tm^2	67
Figure [5.1.3]: Upper Bounds: Neutrino Magnetic Moment vs Tm^2	68
Figure [5.1.4.a]: Upper Bounds: Electron Neutrino Magnetic Moment vs Tm^2	69
Figure [5.1.4.b]: Upper Bounds: Muon Neutrino Magnetic Moment vs Tm^2	69
Figure [5.1.4.c]: Upper Bounds: Tau Neutrino Magnetic Moment vs Tm^2	70
Figure [5.1.5]: Lower Bounds: Neutrino Magnetic Moment vs Tm^2	72
Figure [5.1.6.a]: Lower Bounds: Electron Neutrino Magnetic Moment vs Tm^2	72
Figure [5.1.6.b]: Lower Bounds: Muon Neutrino Magnetic Moment vs Tm^2	73
Figure [5.1.6.c]: Lower Bounds: Tau Neutrino Magnetic Moment vs Tm^2	73

INTRODUCTION

The magnetic moment of a particle is an intrinsic property of charge and depends on the quantity of mass. Magnetic moment plays an important role in describing the interaction of particles with their surroundings. Behavior of matter and its interactions at extremely high temperatures have important implications in astrophysics and cosmology. This involves studying the coupling of charge with the magnetic field using basic concepts of quantum electrodynamics (QED). Quantum field theory (QFT) is the relativistic quantum mechanics of particles and their mutual electromagnetic interactions given by QED. It deals with the dynamics of relativistic moving particles. It is used for detailed study of the coupling of particles with magnetic field. In this thesis we use various methods of renormalization scheme of QFT to thoroughly recalculate the magnetic moment of different particles in vacuum and then study the finite temperature corrections from the hot medium [7-11, 30-34]. The results enable us to select the best ways to uncover the details of these physical systems. This thesis mainly focuses on calculating thermal corrections to determine the sensitivity and impact to the early universe.

Magnetic moment is a quantity that determines the torque experienced by charged particles in a magnetic field. This means that the reaction between the particle and magnetic field is determined by the magnetic moment. There are two types of magnetic moments that can occur. The first one is called intrinsic magnetic moment and is related to the intrinsic spin of a charged particle and its coupling with the magnetic field. Neutral particles can only exhibit induced magnetic moment when they couple with a charged particle through virtually emitted charged particles. This occurs when a virtual charged particle induces a magnetic moment to a coupled real particle. This kind of induced magnetic moment is a higher order effect and is related to the spin of the charged particle.

The magnetic moment is an important quantum mechanical quantity and is needed to understand the interaction of particles with their surroundings. Understanding the behavior of matter and its interactions has important implications in multi-particle systems. It is important to calculate the induced magnetic moment using the basic concepts of QED when studying the coupling of particles with magnetic fields.

Magnetic moment is measured in units of Bohr magneton and is expressed as μ_B . This is equal to the intrinsic magnetic moment of an electron in units of the magnetic field and is defined as:

$$\mu_B = \frac{e\hbar}{2m_e} \quad [0.1.1]$$

One Bohr magneton is the magnetic moment of an electron in a magnetic field and is calculated as a spin effect in quantum mechanics. The spin of a particle is its intrinsic angular momentum. All fermions have a spin equal to an integral multiple of $\frac{1}{2}\hbar$ and bosons have integral spin including spin zero. When a particle interacts with a magnetic field, a torque is applied to the particle. It is a perturbative effect and we would not be able to understand magnetic moment without quantum mechanics.

Perturbation theory of quantum mechanics helps to understand the basic concepts of magnetic moment. QED is considered the simplest gauge theory in explaining the interactions between light and matter. It incorporates thermal medium effects through the self-mass and self-energy corrections and vacuum fluctuations of particle propagators in the background of particles that exist in the heat bath [24-34]. Within this heat bath, virtual particles are created and annihilated at high energies. Perturbation theory of QED plays a vital role when calculating the magnetic moment at finite temperature.

Scientists have calculated the number of neutrinos that should be emitted from the Sun, but found that detectors on Earth were measuring far fewer neutrinos than were

theoretically calculated. This came to be called the Solar Neutrino Problem. Many scientists have worked to figure out this issue and the common solution is neutrino mixing and oscillation. It has been discovered that the flavor of the neutrino changes between the emitted source and detection [37-39]. This can only happen if neutrinos have mass. This means that the predicted Standard Model value of neutrinos being massless was wrong. Therefore, we use an extended version of the minimal standard model for our magnetic moment calculations. Neutrino oscillation and mixing is now a common theory and massive neutrinos need to be included in calculations for accuracy.

CHAPTER I: MOTIVATION

The magnetic moment of a particle is the ability of interaction of a particle's charge with the magnetic field. The magnitude of magnetic moment is proportional to the mass of the particle [1-3, 16, 18-26]. Therefore, charge and mass are both required parameters to describe intrinsic magnetic moment. Molecules, being electrically neutral, have a magnetic moment and can behave as dipoles. For example, differences in atomic mass produces different effects in the same magnetic field on differently charged particles inside atoms. This results in the net nonzero magnetic moment. So, the composite structures acquire magnetic moment due to the variation in mass even if the charge is neutralized. Molecules or electrically neutral particles can behave as dipoles with two equal and opposite charges. Dipoles exhibit nonzero magnetic moment of electrically neutral composite molecules, which applies to neutral composite particles like neutrons as well. This realization led scientists to discover that an electrically neutral composite system acquires a small magnetic moment due to the non-uniform distribution of mass and charge. Electrons and protons have intrinsic magnetic moment, whereas neutron magnetic moment is contributed because neutrons have three constituent quarks. These quarks carry individual magnetic moment that adds up to a net magnetic moment to neutrons. Molecules may have a larger mass distribution of charges to acquire magnetic moment.

We focus on leptons only because they are strongly affected by the temperature of the medium and chemical potential. This is because they are lightest in mass and carrying charge. The main objective of this thesis is the investigation of temperature effects of astrophysical media on the magnetic moment. For this study we apply the renormalization techniques of QED at finite temperature. The thesis will thoroughly

explain a relationship between necessary variables within each equation and find answers for why they interact in a specific way. The applications of how finite temperature effects magnetic moment and the propagation of particles in astrophysical and cosmological environment are studied in detail as well.

The induced magnetic moment of the neutrino is a relatively distinct feature as neutrinos are point particles that are neutral. The intrinsic magnetic moment of neutrino is essentially zero because of neutrality. However, considering the neutrino mass models [33, 38, 44], the extremely light neutrinos may show some indirect effect of induced magnetic moment on some measurable quantities. Therefore, the calculation of magnetic moment of neutrino induced by the corresponding same generation leptons is worth calculating. The magnetic moment of leptons is an important feature for leptons because of their light masses.

This thesis includes a description of magnetic moment and a review of its calculation schemes in quantum mechanics and QED, generalizing it to finite temperature. For quantum statistical field theory, we will use the real-time formalism in Minkowski space. Then, the magnetic moment of different particles at $T=0$ will be calculated and the relevance of mass for the calculation of magnetic moment will be discussed. It has been calculated in literatures explicitly that the effective value of mass changes with temperature [19-22].

In this thesis we show the effect of temperature on the magnetic moment of different types of leptons in relevant media. The focus will be a comparative study of the magnetic moment of leptons from all three generations. We will mention some of the applications of the calculations of magnetic moment to astrophysics and cosmology. This includes the thermal effects on magnetic moment and mass of certain astrophysical systems such as the early universe, neutron star cores, and supernovae.

It is important to fully understand the magnetic moment of particles to determine the effect of magnetic field on any system. The thesis will expand our knowledge on this topic by calculating the magnetic moment of charged leptons and neutrinos. In the beginning, we will carefully review the vacuum calculations of magnetic moment and then will discuss the methods of evaluation of temperature effects on the magnetic moment. We plan to explicitly discuss each case where temperature influences the corresponding quantities (at T=0) and where thermal effects are non-negligible. Then, we will study more complex cases that involve a relationship between mass and magnetic moment of each particle as well as their interaction in a hot medium [7-11 30-34]. These calculations will prove to be helpful in different ways and show its many applications in the universe.

Development of Quantum Field Theory

The Schrodinger equation is the basic equation of motion of particles in non-relativistic quantum mechanics [13, 40, 42] and is given as:

$$-\frac{\hbar^2}{2m}\nabla^2\psi + V\psi = i\hbar\frac{\partial\psi}{\partial t} \quad [1.2.1]$$

This equation represented the time (t) dependent wave function, $\psi(r, t)$ as a function of special coordinates. The vector \mathbf{r} corresponds to three-dimensional vector and m is the mass of the particles with the potential energy, V. These particles correspond to state functions and obey the corresponding uncertainty principle.

$$\Delta x \Delta p_x \sim \hbar \quad [1.2.2]$$

Quantum mechanics leads to the quantization of angular momentum of particles and describes the atomic structure in detail. Non-relativistic quantum mechanics gives a complete description of atomic structure and the atomic reactions using the intrinsic

magnetic moment of electron. It also provides a detailed understanding of atomic bonding and molecular formation. However, the physics of fundamental particles is not well-understood by quantum mechanics alone. For a deeper understanding of the dynamics of these subatomic particles, we must treat them as relativistic particles in a 4-dimensional representation. We also must include particles spin statistics and adopt a field theoretic approach for relativistic subatomic systems.

In relativistic quantum mechanics, particles are moving so fast that we are not able to measure the momentum or the position of the particles. This is because in relativistic quantum mechanics, particles become a quantized field. This means we can measure the region the particles are in, but we are not able to measure them precisely. The region is quantized which means the particles could be anywhere in the region or the associated field. This also means that when particles interact, it does not actually mean they are colliding. It means their fields are interacting with one another.

The first important equation in relativistic quantum mechanics is the relativistic energy momentum relation. This is also called the Klein-Gordon equation for a scalar particle state ϕ .

$$-\frac{1}{c^2} \frac{\partial^2 \psi}{\partial t^2} + \nabla^2 \psi = \left(\frac{mc}{\hbar}\right)^2 \psi \quad [1.2.3]$$

The Klein-Gordon equation works perfectly fine with integral spin particle bosons including scalars particles with zero spin such as the neutral Higgs Boson H^0 . Particles with half integral spin obey Fermi-statistics and obey the Dirac equation instead.

$$(\not{\partial} + m)\psi = 0 \quad [1.2.4]$$

ψ is a 4-dimensional state function with two Dirac spinors: indicating two spin states for each particle and antiparticle. This is different from 4-vector, which correspond

to four basis vectors which generate a vector space [17]. A 4-dimensional representation of gamma matrices constructed from the Pauli spin matrices is given as:

$$\gamma^0 = \begin{pmatrix} I_2 & 0 \\ 0 & -I_2 \end{pmatrix}, \gamma^k = \begin{pmatrix} 0 & \sigma^k \\ -\sigma^k & 0 \end{pmatrix}, \gamma^5 = \begin{pmatrix} 0 & I_2 \\ I_2 & 0 \end{pmatrix}, \quad [1.2.5]$$

with Pauli spin matrices given as,

$$\sigma_1 = \sigma_x = \begin{pmatrix} 0 & 1 \\ 1 & 0 \end{pmatrix}, \sigma_2 = \sigma_y = \begin{pmatrix} 0 & -i \\ i & 0 \end{pmatrix}, \sigma_3 = \sigma_z = \begin{pmatrix} 1 & 0 \\ 0 & -1 \end{pmatrix} \quad [1.2.6]$$

which, gives the detailed form of gamma matrices with peculiar well-known properties as:

$$\begin{aligned} \gamma^0 &= \begin{pmatrix} 1 & 0 & 0 & 0 \\ 0 & 1 & 0 & 0 \\ 0 & 0 & -1 & 0 \\ 0 & 0 & 0 & -1 \end{pmatrix} & \gamma^1 &= \begin{pmatrix} 0 & 0 & 0 & 1 \\ 0 & 0 & 1 & 0 \\ 0 & -1 & 0 & 0 \\ -1 & 0 & 0 & 0 \end{pmatrix} & [1.2.7] \\ \gamma^2 &= \begin{pmatrix} 0 & 0 & 0 & -i \\ 0 & 0 & i & 0 \\ 0 & i & 0 & 0 \\ -i & 0 & 0 & 0 \end{pmatrix} & \gamma^3 &= \begin{pmatrix} 0 & 0 & 1 & 0 \\ 0 & 0 & 0 & -1 \\ -1 & 0 & 0 & 0 \\ 0 & 1 & 0 & 0 \end{pmatrix} \end{aligned}$$

The relativistic generalization of the Schrodinger equation in Klein-Gordon and Dirac equations, based on spin, builds a foundation for quantum field theory. These equations incorporate spin statistics which gives a guideline to develop different rules to represent interaction of particles. Diagrammatic representation of these rules is given by Feynman diagrams. The wavefunction ψ can be represented as a two-dimensional column vector, where u corresponds to particle spinor and v to the antiparticle spinors and each one of them bears two spin states: spin up ($s= +1/2$) and spin down ($s= -1/2$).

In order to move ψ from one state to another, we need to introduce the scattering matrix, S-matrix. This is a matrix giving a transition of an initial state to a final

state of a physical system when it is undergoing scattering. An experimental physicist will run an experiment where the incoming particle is at $t \rightarrow -\infty$. They will then measure the outgoing particle at $t \rightarrow +\infty$ and see the result. What happens in between these measurements is considered the probability amplitude, or the S-matrix:

$$S_{\beta\alpha} = (\Psi_{\beta}^{-}, \Psi_{\alpha}^{+}) \quad [1.2.8]$$

The S-matrix is used in quantum mechanics to describe a physical process shown in Feynman diagrams. Feynman rules in quantum field theory (QFT) are used to write a matrix element for a given QFT process from the corresponding Feynman diagram [13, 40, 42]. Feynman diagrams will be explained in more detail later in this thesis.

Expanding the S-matrix from above is equal to:

$$S = a_{+} + a_{-}\gamma^0\gamma^1 = \begin{pmatrix} a_{+} & a_{-}\sigma_1 \\ a_{-}\sigma_1 & a_{+} \end{pmatrix} = \begin{pmatrix} a_{+} & 0 & 0 & a_{-} \\ 0 & a_{+} & a_{-} & 0 \\ 0 & a_{-} & a_{+} & 0 \\ a_{-} & 0 & 0 & a_{+} \end{pmatrix} \quad [1.2.9]$$

In this matrix, $a_{\pm} = \pm \sqrt{\frac{1}{2}(\gamma \pm 1)}$ and $\gamma = \frac{1}{\sqrt{1-\frac{v^2}{c^2}}}$. We find out that this is not

invariant, so we need to manipulate it to make it invariant. Introducing the adjunct spinor for $S^{\dagger}\gamma^0S = \gamma^0$. So, an invariant equation for a relativistic system is given by:

$$(\bar{\psi}\psi)' = (\psi')^{\dagger}\gamma^0\psi' = \psi^{\dagger}S^{\dagger}\gamma^0S\psi = \psi^{\dagger}\gamma^0\psi = \bar{\psi}\psi \quad [1.2.10]$$

A parity transformation is when the sign is flipped for spatial coordinates. It looks like this:

$$P: (x, y, z) \rightarrow (-x, -y, -z) \quad [1.2.11]$$

The above equation shows that $\bar{\psi}\psi$ is invariant under the parity transformation and is a true scalar because it does not switch signs. The coordinates that change signs are

called pseudoscalars because of their behavior under parity. Pseudoscalars are created by including γ^5 in the equation. γ^5 is the product of all four of the Dirac (or gamma) matrices to show vectors in Minkowski space-time and can be written as,

$$\gamma^5 = i\gamma^0\gamma^1\gamma^2\gamma^3 = \begin{pmatrix} 0 & 0 & 1 & 0 \\ 0 & 0 & 0 & 1 \\ 1 & 0 & 0 & 0 \\ 0 & 1 & 0 & 0 \end{pmatrix} \quad [1.2.12]$$

Adding in γ^5 with the relativistic invariant equation becomes,

$$(\bar{\psi}\gamma^5\psi)' = -\psi^\dagger\gamma^0\gamma^5\psi = -(\bar{\psi}\gamma^5\psi) \quad [1.2.13]$$

This shows that adding in the gamma matrix makes the scalar change signs, becoming a pseudoscalar. This same principle can be used with vectors as well. All the interactions in quantum field theory are described combining state vectors and the gamma matrices with the basic properties of particles.

After solving for the Klein-Gordon equation and the Dirac equation, the next logical step is to move on to quantum field theory. Quantum field theory was created as a way to combine quantum mechanics and relativity. The first successful theory within quantum field theory is quantum electrodynamics. In the next chapter we discuss quantum electrodynamics (QED) which is a true interaction theory of electrodynamics at small scales and in an interacting statistical medium.

Quantum Electrodynamics

QED is a quantum mechanical approach to describe the electromagnetic interaction. This is a well-recognized and tested quantum field theory that involves all electromagnetic phenomena. QED is a combination of electrodynamics, quantum mechanics, and relativity. All of these are necessary to create this quantum field theory. In classical electrodynamics, charges interact obeying Coulomb's law and the flow of

charge conservation is indicated by the continuity equation. Classical electrodynamics works very well for 3-dimensional space. For non-relativistic moving particles, classical electrodynamics does not work well and we must move to relativistic quantum mechanics and the quantum field theory of electromagnetic interaction as expressed in QED. In QED, the Coulomb interaction is combined with the Schrodinger equation for a relativistic system and is described in terms of the field theory of electrodynamics. QED is the most well-known theory among all the interacting field theories and is the most tested theory. The Lagrangian equation for QED describes the motion between the electromagnetic field, A_μ and the field of electrons, ψ . The Lagrangian of electromagnetic interaction is given by,

$$\mathcal{L} = -\frac{1}{4}F_{\mu\nu}F^{\mu\nu} + \bar{\psi}(i\partial - m)\psi + eA_\mu \times \bar{\psi}\gamma^\mu\psi \quad [1.3.1]$$

The electromagnetic processes among interacting particles are given by Feynman diagrams. Each term in this QED Lagrangian correspond to segments of the Feynman diagram. The probability of interaction in all field theories are calculated from the Feynman diagrams using Feynman rules.

Feynman diagrams are often used to convey the QED principles by translating the QED equations into Feynman diagrams [17]. To demonstrate an electron propagator, we use the usual notation of QED. The propagator of the charged fermion is shown in the figure below and the direction of the momentum p is represented by the direction of the arrow.

$$\psi \xrightarrow[p \longrightarrow]{} \bar{\psi} = \frac{i}{\not{p} - m + i0} \quad [1.3.2]$$

Photon propagators are shown with a wavy line and the corresponding propagator of the equation is given as,

The last term, $eA_\mu \times \bar{\psi}\gamma^\mu\psi$ represents the perturbative effects in QED. In quantum mechanics, perturbation theory is a set of approximation equations used to represent a small variation in energy in a quantum mechanical system, referred to as radiative corrections. These variations are complicated and usually small. Certain techniques of perturbation theory make them simpler in mathematical terms. It does this by adding corrections to the exact Hamiltonian to create approximate solutions. Perturbation is a very important topic of quantum mechanics as well as field theory and will be discussed later in more detail.

Feynman Diagrams in QED

Feynman diagrams are used in quantum field theory to describe particle processes. Interaction of these particles can be written using the Feynman rules of the corresponding theory. Feynman diagrams are diagrammatic representation of particle processes in different interactions. Each part of the diagram can be expressed in terms of Feynman rules. Matrix elements for these processes are written using Feynman rules. The square of the matrix elements, integrated over the phase space, gives the probability of particle processes. QED is a well-known field theory and the matrix element of any QED process can be written using the Feynman rules. The square of the matrix element is summed over initial states and averaged over the final states to integrate over the available phase space. To fully understand Feynman diagrams, the Feynman rules of QED are discussed in detail [17]. The basic variables used for Feynman diagrams in QED are as follows:

Table [1.4.1]: Feynman Diagram Rules

Particle	Feynman Rule
Ingoing fermion	u
Outgoing fermion	\bar{u}
Ingoing antifermion	\bar{v}
Outgoing antifermion	v
Ingoing Photon	ϵ^μ
Outgoing Photon	$\epsilon^{\mu*}$
Ingoing scalar	1
Outgoing scalar	1

Each external line has momentum p , which can be distinguished as p_1, p_2, \dots, p_n and the internal lines each have a momentum q corresponding to each line given as q_1, q_2, \dots, q_n . These momenta are important to describe the propagator and vertex equations. The next important piece of the diagram is the vertex function. The QED vertex is an intersection of three points where two charged particles interact with each other through a photon. The vertex contributes a factor $ig_e \gamma^\mu$ that is proportional to the electromagnetic coupling g_e . This coupling is a vector in nature. In this equation, the coupling constant g_e is a dimensionless quantity and is related to electron charge: $g_e = e \sqrt{\frac{4\pi}{\hbar c}}$. The speed of light c in a natural system of units satisfy the condition, $c = \hbar = k_B = 1$ and is used to describe the Feynman rules of QED.

Another important component of a Feynman diagram is a propagator. The propagators are different for different types of particles. The fermion propagators representing both electrons and positrons can be written in terms of their momenta p as,

$$\frac{i(\not{p} \pm m)}{p^2 - m^2} \quad [1.4.1]$$

On the other hand, the propagator equation for photons is equal to:

$$\frac{-ig_{\mu\nu}}{q^2} \quad [1.4.2]$$

The next part to address is conservation of momentum and energy. This needs to be added to each vertex to show this law of conservation is being observed.

$$(2\pi)^4 \delta^4(k) \quad [1.4.3]$$

To show this, we use a delta function where k indicates four-momentum of a photon going into the vertex. This k should be subtracted if the arrows lead outwards. P is the 4-momentum of an electron and the overall contributions can be obtained by integrating the matrix element over the phase space factor of each fermion momentum p . For each momentum that is internal, p , in the diagram, integrate over the equation below:

$$\frac{d^4p}{(2\pi)^4} \quad [1.4.4]$$

In the end, the factor that represents the conservation of energy and momentum is canceled with the delta function.

$$(2\pi)^4 \delta^4(p) \quad [1.4.5]$$

Multiply this equation by i and what will be left is \mathcal{M} , which is the amplitude.

Decay Rates and Cross-sections

Feynman rules are used to calculate the probability of electromagnetic processes using matrix elements. The calculation of decay rates and cross-sections is the most important part of these processes. We give a few examples of the Feynman diagrams below to demonstrate the calculational procedure, first in vacuum and then at finite

temperatures. Feynman rules remain unchanged in statistical background. Just to understand the applications of Feynman rules, we consider an example of a decay rate. For this purpose, we consider the simplest decay process $Z^0 \rightarrow l^+ l^-$ and the Feynman diagrams of this decay process are given as:

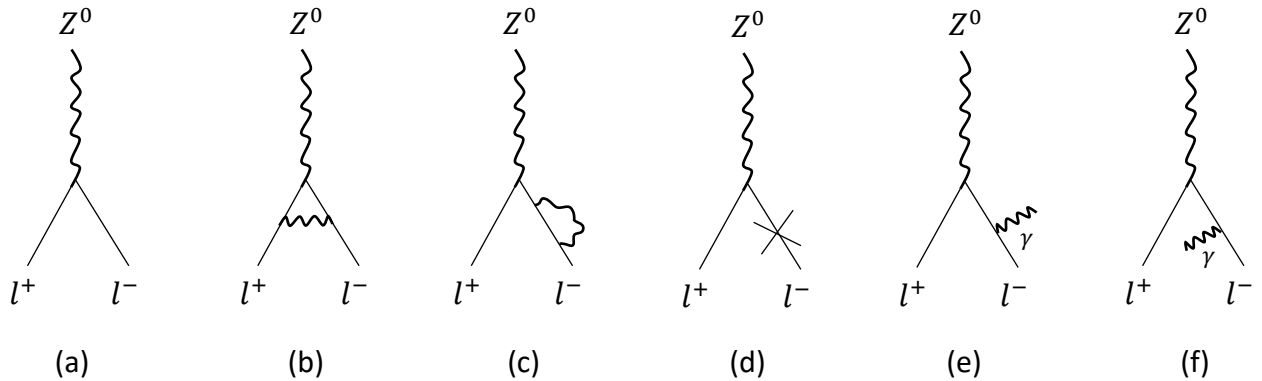


Figure [1.5.1]: Radiative Corrections for Decay of $Z^0 \rightarrow l^+ l^-$
 (a) is a basic tree level diagram without radiative corrections, (b) corresponds to the vertex correction, (c) the self-mass correction, (d) the counterterm and (e) and (f) indicate the Bremsstrahlung emission and absorption, respectively.

The decay rate of the first order radiative corrections can be calculated using the above diagrams of Figure [1.5.1]. These diagrams may give infinite decay rate. However, the calculation of the contribution to decay rate from each diagram is added together to cancel singularities. The procedure of order by order cancellation of singularities in a physical process is established through renormalization and the scheme of calculations is called the renormalization scheme [30]. The first Fig. (a) is a tree level diagram which has no radiative corrections, whereas the rest of the diagrams contribute radiative corrections. Fig. (b) represents the vertex corrections. All the radiative correction terms in vacuum are added together in the order α . The vertex correction is an important part that corresponds to the wavefunction. Fig. (c) corresponds to the self-mass correction which means it takes into account virtual particles. Virtual particles are emitted and reabsorbed

by the particle and are considered self-mass because its mass comes from the particle. Virtual particles cannot be directly detected and we only know they exist because of the ability to indirectly observe them through self-mass. Fig. (d) indicates the mass counterterm. The counterterm contributes to the half of the self-mass correction which corresponds to the Feynman diagram that should have propagated, but it never did. This leaves the remaining diagram with infinities that needs to be renormalized to become finite.

Figs. (e) and (f) correspond to the Bremsstrahlung radiation emission and absorption, respectively. This radiation is when the vertex correction breaks off on one side and becomes either emitted or absorbed radiation. The propagator for a massive scalar in vacuum is given as:

$$\frac{1}{Q^2 + M^2 c^2} \quad [1.5.1]$$

Where Q^2 represents the 4-momentum and M represents the mass of the scalar particle exchanged. This is the most basic form of the Feynman propagator.

Fig. (a) represents the basic decay in a vacuum of the Z boson into both a lepton and corresponding anti-lepton. The matrix element for the vertex function of this decay is given as:

$$M_0^\mu = -i\bar{u}(p)\gamma^\mu(g_V - g_A\gamma_5)v(p') \quad [1.5.2]$$

This equation can be explained using the above rules, \bar{u} represents the outgoing lepton, the middle represents the point of decay, and the end equals the anti-lepton's path.

Fig. (a) is the only diagram contributing at low energy in vacuum theory. The other figures are all radiative corrections which corresponds to higher energies.

Background corrections are incorporated through the radiative corrections and contribute at higher energies only.

Renormalization of QED

Renormalization is an important tool to check the validity of gauge theory for a physically interacting system. Renormalizability of QED in vacuum is well-established. While incorporating statistical corrections, a test of renormalizability is required. The renormalizability of QED at finite temperature has been checked explicitly and the renormalization constants of QED have explicitly been calculated in a real-time formalism [14-16]. Real-time formalism of finite temperature field theories is used to calculate the renormalization of QED. In the presence of renormalization constants, the Lagrangian remains invariant under gauge transformation. All the infinities of QED Lagrangian are cancelled for each individual order of perturbation due to the renormalizability of the theory. All the infinities of the gauge theories are removed at each order of perturbation. The three key quantities are mass, wavefunction, and charge. These correspond to the renormalization operators that are present in QED. In Gunnar Källén's paper, he uses the constants K, L, and N for these operators. K corresponds to the renormalized mass, L corresponds to renormalized charge, and N corresponds to renormalized wavefunction [15]. These values are renormalized by adding all the same order terms in the Lagrangian.

To add these extra terms, we turn the 4-dimensional Schrodinger equations for spin $\frac{1}{2}$ particles into Dirac equations for both particles and antiparticles. The Dirac equation for spin $\frac{1}{2}$ fermions is written as:

$$i \left(\gamma^0 \frac{\partial \psi}{\partial t} + \vec{\gamma} \vec{\nabla} \psi \right) - m \psi = 0 \quad [1.6.1]$$

For antiparticles, the Dirac equation is given as,

$$i \left(\frac{\partial \psi}{\partial t} \gamma^0 + \vec{\nabla} \psi^+ (-\vec{\gamma}) \right) + m \psi^+ = 0 \quad [1.6.2]$$

This turns the QED Lagrangian into,

$$\mathcal{L}_{QED} = i\hbar c \bar{\psi} \mathcal{D} \psi - mc^2 \bar{\psi} \psi - \frac{1}{4\mu_0} F_{\mu\nu} F^{\mu\nu} \quad [1.6.3]$$

This equation explains the electromagnetic particle processes in 4-dimensional space. The represented tree diagram for decay in Fig. (a) has a matrix element which corresponds to the wavefunction. When taking the absolute value of this matrix element and squaring it, we can find out the probability of this particle interaction. Taking the integral of this probability results in the calculation of the cross-section of the decay. Each diagram in Figure [1.5.1] corresponds to one part of renormalization. They each add an additional term to the Lagrangian to create a total value of how QED is affected by perturbation theory and needs to be renormalized. The radiative corrections in a majority of the figures are explained in the following section.

Radiative Corrections at Finite Temperature

The Feynman rules of vacuum theories can be used at finite temperature by replacing the vacuum propagators with thermal propagators. The fermion propagators represent the fermions that are present in the background and contribute to the radiative corrections on the matrix element. The fermion propagator at finite temperature and density is represented by the equation:

$$S_{\beta}(p) = \frac{i(\not{p} + m)}{p^2 - m^2 + i\epsilon} - 2\pi(\not{p} - m)\delta(p^2 - m^2)n_F(p \pm \mu) \quad [1.7.1]$$

With μ representing the chemical potential of a highly dense system. The number of bosons that are present in the background are also important. They effect the equation of

the vertex and matrix element as well, but in a slightly different way. This is represented by the equation below:

$$D_{\beta}^{\mu\nu}(k) = -g^{\mu\nu} \left[\frac{i}{k^2 + i\epsilon} + 2\pi\delta(k^2 - m^2)n_B(k) \right] \quad [1.7.2]$$

Where β represent the inverse temperature. Within these equations the terms below represent the distribution of each of these particles in the background. The fermion distribution function is represented by the Fermi-Dirac distribution.

$$n_F(p \pm \mu) = \frac{1}{e^{\beta(|p \cdot u| \pm \mu)} + 1} \quad [1.7.3]$$

and the boson distribution function is represented by Bose-Einstein distribution function.

$$n_B(k) = \frac{1}{e^{\beta|k \cdot u|} - 1} \quad [1.7.4]$$

For Fig. (b), the matrix element takes into account the fermion and boson propagators present in the background affecting the heat bath. It is clearly seen below that the equations of the propagators are present. The vertex function gives the exchange of virtual photons between fermion legs. We replace the vacuum propagators by the thermal propagators in the above diagrams to give the matrix element of the decay process as:

$$M_v^u = -ie^2 \bar{u}(p) \int \frac{d^4k}{(2\pi)^4} g^{\alpha\beta} \gamma_{\alpha} \left[\frac{i}{k^2 + i\epsilon} + 2\pi\delta(k^2)n_B(k) \right] (\not{p} - \not{k} + m_l) \gamma^{\mu} \times \left[\frac{i}{(p-k)^2 - m_l^2 + i\epsilon} - 2\pi\delta((p-k)^2 - m_l^2)n_F(p-k \pm \mu) \right] \times (g_v - g_A \gamma_5) (\not{p}' - \not{k} + m_l) \times \left[\frac{i}{(p'-k)^2 - m_l^2 + i\epsilon} - 2\pi\delta((p'-k)^2 - m_l^2)n_F(p'-k \pm \mu) \right] \gamma_{\beta} v(p') \quad [1.7.5]$$

Fig. (c) takes into account the self-energy of the lepton. This refers to the emission and reabsorption of a virtual photon. This short-lived virtual photon cannot be directly detected, but its correction to the decay rate make it clear that this self-energy contribution is nonzero. This is represented in the matrix element equation given as:

$$M_{SE}^\mu = -i\bar{u}(p) \left[\gamma^\mu (g_V - g_A \gamma_5) \left(\frac{\delta m_l}{p+m_l} - \frac{\alpha}{4\pi^2} \frac{\int_0^\infty \left(\frac{dk}{k}\right) n_B(k)}{2m_l} + \frac{\alpha}{4\pi^2} 8\pi \int_0^\infty \left(\frac{dk}{k}\right) n_B(k) \right) + \left(\frac{\alpha}{4\pi^2} 8\pi \int_0^\infty \left(\frac{dk}{k}\right) n_B(k) + \frac{\delta m_l}{p-m_l} - \frac{\alpha}{4\pi^2} \frac{\int_0^\infty \left(\frac{dk}{k}\right) n_B(k)'}{2m_l} \right) \gamma^\mu (g_V - g_A \gamma_5) \right] v(p') \quad [1.7.6]$$

Similar to the emission of virtual photons in Fig. c, the negative term in the matrix element for self-mass is given by the mass counterterm. This is similar to the previous diagram's matrix element, but the self-mass is calculated from the surrounding particles contributing to the mass of the lepton. This adds additional factors to the matrix element equation as well as the other electromagnetic properties.

$$M_{CT}^\mu = -i\bar{u}(p) \left[\gamma^\mu (g_V - g_A \gamma_5) \left(-\frac{\delta m_l}{p+m_l} + \frac{\alpha}{2\pi^2} \frac{\int_0^\infty \left(\frac{dk}{k}\right) n_B(k)}{2m_l} \right) + \left(-\frac{\delta m_l}{p'-m_l} + \frac{\alpha}{4\pi^2} \frac{\int_0^\infty \left(\frac{dk}{k}\right) n_B(k)'}{2m_l} \right) \gamma^\mu (g_V - g_A \gamma_5) \right] v(p') \quad [1.7.7]$$

The matrix element for the emission of Bremsstrahlung radiation is given by the following equation:

$$M_{RE}^\mu = -ie\bar{u}(p) \left\{ \left[\left(\frac{p'^\nu}{p' \cdot k} - \frac{p^\nu}{p \cdot k} \right) \gamma^\mu + \frac{\gamma^\nu k}{2} \left[\frac{1}{p \cdot k} + \frac{1}{p' \cdot k} \right] \right] \gamma^\mu \varepsilon_\nu - \frac{(k^\mu \varepsilon - k \varepsilon^\mu)}{p' \cdot k} \right\} (g_V - g_A \gamma_5) v(p') \quad [1.7.8]$$

This equation is the same for the absorption of Bremsstrahlung radiation except the value of k^μ is changed to negative.

Renormalization in QED in Finite Temperature

Renormalization at finite temperature is essential when calculating the effects of particles in hot and dense media using quantum field theory. We use the real-time formalism to calculate the background contributions throughout the particle processes [1-3, 20-22]. Renormalization is used as a technique in many different equations to unveil finite solutions to problems that were previously infinite. It has been used in the self-mass

of electrons and decay rates. The renormalization for QED at finite temperature is a well-studied topic [23-29]. Scientists have solved for various temperatures and chemical potentials. These all correspond to various conditions of astrophysical phenomena throughout the universe. The calculations for the largest values of chemical potential (where chemical potential is greater than both mass and temperature) simulate the conditions for highly dense compact systems such as neutron stars and supernovae. For this case, the photons in the background are ignored because they do not contribute to chemical potential due to the photon having no mass.

The electron self-energy needs to be calculated using renormalization techniques to solve the effect of photons on charged particles [25]. We use the example of the self-energy of an electron. $G_F(p)$ is the electron propagator and using perturbation theory, we can calculate the Feynman Green theory correction. m_0 and e_0 represent the bare minimum charge and mass of the electron. The following Feynman diagrams contribute to the first order radiative corrections to self-mass of electron.

$$G_F(p) = \text{---} \leftarrow \text{---} + \text{---} \leftarrow \text{---} + \mathcal{O}(\epsilon_0^4) = \frac{i}{\not{p} - m_0 + i\epsilon} + G_F^{(1)}(p) + \mathcal{O}(\epsilon_0^4)$$

[1.8.1]

The self-mass of the particle is included with this diagram. This is added to the equation in combination with the electron mass, which computes the self-mass corrections and is equal to the effective mass. The self-energy of the photon propagator is included in the equation below and corresponds to the given diagrams [34-35]. These corrections need to be added to the photon to get accurate calculations.

$$(2\pi)^4 \delta^4(k+k') G_{\mu\nu}^F(k) = \mu \text{---} \leftarrow k \text{---} v + \mu \text{---} \leftarrow k \text{---} \begin{array}{c} \text{---} p+k \text{---} \\ \circlearrowleft \\ \text{---} p \text{---} \\ \text{---} \alpha \quad \beta \text{---} \\ \circlearrowright \end{array} \leftarrow k \text{---} v + O(\varepsilon_0^4) \quad [1.8.2]$$

The one-loop diagram for the self-energy of the photon propagator is shown with the below diagram,

$$+ \mu \text{---} \leftarrow k \text{---} \begin{array}{c} \text{---} p+k \text{---} \\ \circlearrowleft \\ \text{---} p \text{---} \\ \text{---} \alpha \quad \beta \text{---} \\ \circlearrowright \end{array} \leftarrow k \text{---} v^- \quad [1.8.3]$$

This diagram explains how the photon propagator is added in as well as the electron charge. This all adds up to contribute to the photon coupling constant, which is necessary for interaction.

The renormalization process will be used in this thesis to calculate the electron self-mass when studying the magnetic moment of electrons. This will be very important to the final result and applications. After summarizing the calculational scheme of the electromagnetic interaction at finite temperature, we discuss neutrinos in the next chapter. We use the calculation scheme to compute the electromagnetic properties of weakly interacting neutral neutrinos.

CHAPTER II:
ELECTROMAGNETIC FORM FACTORS

Dirac Neutrinos

Wolfgang Pauli first proposed the neutrino in 1930 as a way to make up for the missing energy in beta decay. He originally called this particle the neutron, but this did not last long because the name was already taken by a much heavier nuclear particle. Enrico Fermi then came up with the name neutrino in 1932 and then later used it in one of his papers where he used different particles proposed by his fellow colleagues to explain beta decay (positron, neutrino, neutron, and proton).

Neutrinos are fermions that use the weak force to interact. In the standard model they are considered leptons which mean they have spin $\frac{1}{2}$ and do not interact strongly like electrons [43]. In the standard electroweak model, the individual lepton number of neutrinos is conserved, which means it has the same number of leptons and antileptons of the same flavor. The neutrino was originally thought to be massless. Its rest mass is so small that it was thought to be zero for a long time. In the standard electroweak model (SEWM), massless, left-handed neutrinos are named Weyl neutrinos. The minimally extended standard model has one right-handed neutrino with a small mass that behaves as a Dirac particle. However, the massive neutrino, even with a small mass has different properties than Weyl neutrinos.

Electromagnetic form factors are important to all charged particles with electromagnetic interactions. For neutral particles, the form factors are induced as radiative corrections. Electromagnetic form factors are different types of interactions within a region that are predicted to take place by a particle. Fermions with a $\frac{1}{2}$ integral spin are known to have four form factors. These are called charge radius, electric dipole moment, magnetic dipole moment, and anapole moment. The form factors of a neutrino

are calculated from the electroweak (matrix) vertex $\Gamma^\mu(q, l)$ [4, 36]. This vertex relates to the matrix element of the electromagnetic current by the neutrino mass before and after the interaction as well as the 4-momentum (p). All spin $\frac{1}{2}$ particles use the same equation as the basis for their electromagnetic form factors. The starting equation is the matrix element that involves the current in the initial and final states. This equation can be written as:

$$\langle \psi(p_1) | J^\mu(0) | \psi(p_2) \rangle = \bar{u}(p_1) \Gamma^\mu(q, l) u(p_2) \quad [2.1.1]$$

The standard vertex function for the neutrino can then be written as:

$$\bar{u}(p_1) \Gamma^\mu(q, l) u(p_2) = \bar{u}(p_1) \left\{ F_1(q^2) \gamma^\mu - \frac{i\sigma^{\mu\nu}}{2m} q_\nu F_2(q^2) + i\epsilon^{\mu\nu\alpha\beta} F_3(q^2) \frac{\sigma_{\alpha\beta}}{4m} q_\nu + \frac{1}{2m} (q^\mu - \frac{q^2}{2m} \gamma^\mu) \gamma_5 F_4(q^2) \right\} u(p_2) \quad [2.1.2]$$

In this equation, $F_{1,2,3,4}$ represent the charge radius, magnetic dipole moment, electric dipole moment, and anapole moment respectively. The following sections go into further detail on each of these form factors. The equation, $q = p_i - p_f$, is the four-vector momentum before and after interaction. When calculating these form factors, $q^2 = 0$ will be used to show the form factors are only interacting with real photons. The matrix γ_5 represents the product of the 4-gamma matrices and is used to describe the axial properties of electroweak interaction through the axial coupling. The gamma matrices are also called Dirac matrices and represent 4 vectors of Minkowski space in electromagnetic interaction. When we calculate the matrix element using the below bubble diagram, the coefficients of different gamma matrices give the contributions of different types of form factors.

Charge Radius

In the minimal standard model, neutrinos are massless and cannot bear any charge. Extending this model to include massive neutrinos means neutrinos can couple with corresponding charged leptons via the bubble diagram. They also can have a charge radius as well as electric and magnetic dipole moments. This is very important in the early universe because particles that have a small electric charge can interact with the surrounding medium [36]. This influences pair production and big bang nucleosynthesis [8]. In the vertex function for the Dirac neutrino, F_1 represents the charge, Q .

$$F_1(0) = Q \quad [2.2.1]$$

This can be shown as the non-relativistic interaction Hamiltonian equation [37],

$$H_{int}^{NR}[F_1] = F_1(0)A_0 \quad [2.2.2]$$

A_0 represents the potential energy of the current at the zeroth component along with the charge.

Another way to express the charge form factor of a neutrino is with the gauge invariant calculation below [43],

$$\langle r_{\nu_l}^2 \rangle = \frac{G_F}{4\sqrt{2}\pi^2} \left[3 - 2 \log \left(\frac{m_l^2}{m_W^2} \right) \right] \quad [2.2.3]$$

Here, G_F is the Fermi coupling constant, m_l is the mass of the corresponding charged lepton, and m_W is the mass of the W boson. When calculated, the charge radius for neutrinos in the electroweak model is extremely small $\sim 4 \times 10^{-33} \text{cm}^2$. The tiny mass of neutrino leads to extremely small values of electric and magnetic dipole moments.

Electric Dipole Moment

In a vacuum at $q^2 = 0$ with real photons in the minimal standard model, the electric dipole moment is present. Nowakowski [36] calculated each of the form factors of the neutrino. The electric dipole moment is calculated below as:

$$-\frac{1}{2m}F_3(0) = d \quad [2.3.1]$$

The non-relativistic interaction Hamiltonian equation is then given by,

$$H_{int}^{NR}[F_3] = -d\boldsymbol{\sigma} \cdot \mathbf{E} \quad [2.3.2]$$

This is similar to the magnetic moment equation, but instead of interacting with the magnetic field, \mathbf{B} , it interacts with the electric field, \mathbf{E} . This value has not been found experimentally yet. This value is very small, so this is expected. The anapole moment is not widely researched because it is specific to weakly interacting particles. There is very little information available as the impact may be small enough to be ignored in most systems.

Anapole Moment

The anapole moment is one of the four form factors that take place at the vertex of a particle's interaction. Anapole moment appears as a coefficient of γ_5 and relates to the electroweak model because it is an axial or pseudo-vector. The electromagnetic interaction uses γ_μ because it is a 4-vector. The anapole moment has unique characteristics compared to the other form factors. For instance, in the interaction Hamilton, you can see that the electric field, \mathbf{E} , or the magnetic field, \mathbf{B} , must be nonzero; otherwise, the anapole moment does not exist [36].

$$H_{int}^{NR}[F_4] = F_4(0)\boldsymbol{\sigma} \cdot \left[\nabla \times \mathbf{B} - \frac{\partial \mathbf{E}}{\partial t} \right] \quad [2.4.1]$$

This means that it is the opposite of the other form factors, so it does not exist at $q^2 = 0$, with real photons. This shows that it is independent of the gauge theory.

When a particle has real form factors at $q^2 = 0$, it is said to have diagonal form factors. A particle can only have off-diagonal form factors, or transition form factors, when $q^2 \neq 0$. The diagonal magnetic and electric dipole moments of particles and antiparticles are the same size, but with different charge (+ or -). This is not the case for the anapole magnetic moment. Both the particles and the antiparticles have the same anapole moment. This means the anapole moment is symmetric for opposite charges. Because of this, the Majorana neutrino has a diagonal anapole form factor even though all the other form factors are transition moments. This is the opposite for Dirac neutrinos where all of the form factors are diagonal except the anapole moment is off-diagonal.

The anapole moment of neutrinos has not been found experimentally. There is a lot more to learn about anapole moment because of its unique characteristics.

Magnetic Dipole Moment of Leptons

Intrinsic magnetic dipole moment is the property of charged particles, so the application of the same phenomenon and similar diagrams give various values of the magnetic moment of different lepton flavors conserving individual lepton flavors on each vertex. A general discussion of the individual form factors can give a comparison of individual lepton magnetic moment, corresponding to each flavor. In this thesis we give a comparison of magnetic moment of different leptons based on the masses of the corresponding leptons and their interaction with the medium.

First Generation Lepton Flavor Electron (e and ν_e)

The magnetic moment of an electron is considered as intrinsic magnetic moment. This happens when a particle's intrinsic spin interacts with an external magnetic field. This is seen in the figure below.

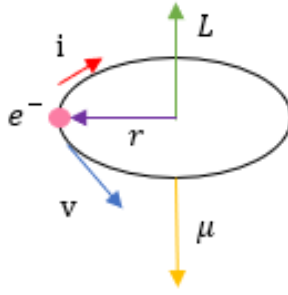


Figure [2.5.1]: Diagram of intrinsic magnetic moment of an electron

This shows if an electron is moving at speed, v , in a circle, with an angular momentum L , it produces a magnetic moment μ in the opposite direction. You can see in this diagram that the dipole moment is equal to current and the area of the circle A such that,

$$\mu = IA \quad [2.5.1]$$

We know that the current in a loop of radius r is equal to:

$$I = \frac{dq}{dt} = \frac{qv}{2\pi r} \quad [2.5.2]$$

Substitution of (2.5.2) into (2.5.1) and setting $A = \pi r^2$ for ($r = r$), we get equation (2.5.3) for the magnetic moment of an electron:

$$\mu = \frac{ev}{2\pi r} (\pi r^2) = \frac{evr}{2} \quad [2.5.3]$$

Compare this to the Bohr magneton and you can see this is a similar equation. It becomes the same equation when you include spin and write it in terms of the angular momentum, L .

The magnetic moment of the electron can be expressed in units of Bohr magneton μ_B , which is defined for spin $\frac{1}{2}$ electron as:

$$\mu_B = \frac{e\hbar}{2m_e} = 5.78 \times 10^{-5} eVT^{-1} \quad [2.5.4]$$

The spin relates to the magnetic moment through its interaction with the magnetic field where it also depends on mass [13, 26, 40].

$$\boldsymbol{\mu} = g\mu_B \mathbf{s} \quad [2.5.5]$$

In this equation, g is the Landé g -factor, which is defined as the ratio of magnetic moment to the angular momentum of a charged particle. This is given as,

$$g\mu_B = \frac{\boldsymbol{\mu}}{\mathbf{s}} \quad [2.5.6]$$

This ratio is used to show the relation between magnetic moment and angular momentum. The g -factor is equal to 2 when using Dirac theory and particles with spin $\frac{1}{2}$.

When using QED, there are more factors involved with electrons that need to be considered. Virtual particles are a large part of electron magnetic moment. Virtual particles are particles that cannot be detected directly. We know they exist because of their measurable indirect qualities. Electrons are constantly surrounded by virtual photons that are being emitted and reabsorbed. This virtual photon cloud adds mass to the electron which is called self-mass.

The self-mass can be determined by calculating the probability of the emission and the absorption of the photons. The coupling equation for this at the moment the magnetic field is applied is below.

$$\alpha = \frac{e^2}{4\pi\hbar c} \quad [2.5.7]$$

This equation is for the emission of one photon. For two photons, the coupling constant needs to be squared, α^2 and so on for more. Feynman diagrams are helpful to

show this phenomenon. The following Feynman diagrams are possible for the emission of photons [40].

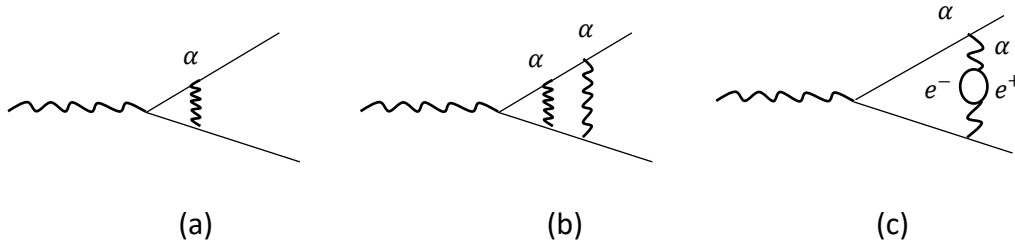


Figure [2.5.2]: Emission and Absorption of Photons
 (a) shows the emission and absorption of one photon. (b) represents the emission and absorption of two photons, (c) represents the virtual particles creates a shield around the electron from external magnetic fields.

This is where renormalization becomes useful with this theory. Renormalization is the process of including all possibilities to cancel singularities by the addition of all same order diagrams. This is cancelled from an infinite answer to get a finite result. The self-energy of the electron would be infinite because there is no limit on the virtual particles' momenta. Renormalization provides a solution to this problem.

When considering the QED type radiative corrections to the electron magnetic moment, we get an equation that is a power series. This is because we are summing up the above Feynman diagrams to calculate a finite answer.

$$\begin{aligned} \left(\frac{g-2}{2}\right)_e^{QED} &= 0.5 \frac{\alpha}{\pi} - 0.32848 \left(\frac{\alpha}{\pi}\right)^2 + 1.19 \left(\frac{\alpha}{\pi}\right)^3 + \dots & [2.5.8] \\ &= (1159652.4 \pm 0.4) \times 10^{-9} \end{aligned}$$

This self-mass is different when evaluated in a hot and dense medium.

Electron Neutrino

Neutrinos can be described in a couple of different ways. One is as a Dirac neutrino and the other is as a Majorana neutrino. The Majorana neutrino only has two distinct states, while the Dirac neutrino has four distinct states. This can be seen below:

$$v^D = \begin{pmatrix} \nu_L \\ \bar{\nu}_L \\ \nu_R \\ \bar{\nu}_R \end{pmatrix} \quad v^M = \begin{pmatrix} \nu_L \\ \nu_R \end{pmatrix} \quad [2.5.9]$$

In the above equations, the L stands for left-handed and the R represents right-handed helicity.

We describe helicity in terms of left or right handedness. Right-handed particles have a spin that is in the same direction as its momentum. Left-handed particle's spin is going in the opposite way of its momentum (or the direction it is moving in). Below is a diagram to show this. S represents the spin of the particle and p represents the momentum.

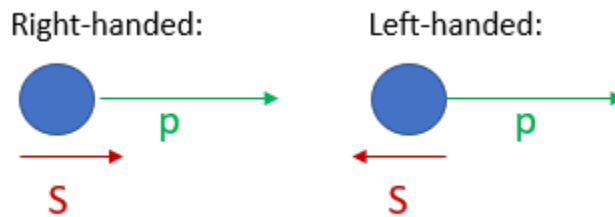


Figure [2.5.3]: The helicity of a particle

For neutrino oscillation to occur, the masses that diagonally correspond to the different neutrino flavors must be different. This means that only Dirac and Majorana type neutrinos can oscillate. Lepton flavor mixing is not allowed in the standard electroweak model. Therefore, we add the right-handed neutrino (also called sterile

neutrino) as an inert particle in the minimally extended standard model. All the Feynman rules of standard electroweak model can still be used [31, 33].

Using the Dirac equation with the Dirac type neutrino and antineutrino, the diagonal magnetic moment can be calculated. This was first done by Lee and Schrock [19] in the 1970s. They expressed the magnetic moment of the massive neutrino (mass is expressed in electron volts) in units of the Bohr magneton μ_B :

$$\mu_\ell^D = \frac{3eG_F m_{\nu_\ell}}{8\sqrt{2}\pi^2} \approx 3.2 \times 10^{-19} \left(\frac{m_{\nu_\ell}}{1\text{eV}} \right) \mu_B \quad [2.5.10]$$

Where,

$$G_F = \frac{\sqrt{2}}{8} \frac{g^2}{m_W^2 c^4} = 1.166 \times 10^{-5} \text{GeV}^{-2} \quad [2.5.11]$$

G_F is the Fermi coupling constant in the weak interaction and m_{ν_ℓ} is the mass of the specific flavor of neutrino, l . The magnetic moment is a very small value, especially when compared to the corresponding charged lepton's magnetic moment.

Using this equation, we use different flavors of the neutrino to calculate the magnetic moment in a vacuum. The masses of different flavors of neutrino are taken from the most up to date experimental results. The upper most bound of the neutrino flavors was found experimentally and recorded by the Particle Data Library [44]. These masses do not follow the standard cosmology model for neutrino mass eigenstates. The masses correspond to the values found in neutrino experiments. Currently the only way to measure neutrino mass is through radiative decay. The detector measures how much energy the corresponding neutrino removed from the charged lepton during radiative decay. This means that with today's detectors, scientists cannot measure the exact mass eigenstates of neutrinos.

There are two different Feynman diagrams we use to explain how the neutral neutrinos interact with the electromagnetic force [31]. It does this by coupling with an

electron and gaining an induced magnetic moment. The bubble diagram below explains this with real particles. The tadpole diagram is another possible way for a neutrino to gain an induced magnetic moment, but this diagram represents probabilities of interacting with virtual particles instead of real ones. We use the bubble diagram in our magnetic moment calculations for this thesis. Both diagrams are portrayed below for the electron neutrino:

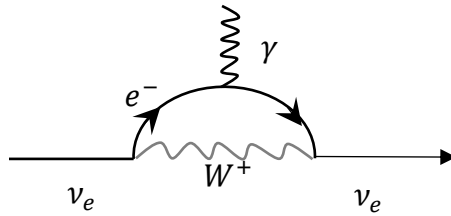


Figure [2.5.4]: Bubble diagram for electron neutrino in the minimal standard model.

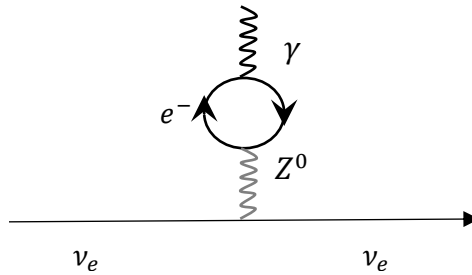


Figure [2.5.5]: Tadpole diagram for electron neutrino in the minimal standard model.

We start with the generalization of Schrock's equation to begin our calculations:

$$\mu_{\nu_\ell}^0 = \frac{3eG_F m_{\nu_\ell}}{8\sqrt{2}\pi^2} = \frac{3m_e G_F m_{\nu_\ell}}{4\sqrt{2}\pi^2} (\mu_B) \approx 3.2 \times 10^{-19} \left(\frac{m_{\nu_\ell}}{1\text{eV}}\right) \mu_B \quad [2.5.12]$$

We replace the general neutrino mass with the specific mass for the electron neutrino. We will first look at the upper bound mass found experimentally [44]:

$$m_{\nu_e} \sim 2.25 \text{ eV}$$

$$\mu_{\nu_e}^0 = \frac{3eG_F m_{\nu_e}}{8\sqrt{2}\pi^2} = \frac{3m_e G_F m_{\nu_e}}{4\sqrt{2}\pi^2} (\mu_B) \approx 7.2 \times 10^{-19} \mu_B \quad [2.5.13]$$

This mass value is too large for early universe calculations because it has been found that the sum of all neutrino mass eigenstates cannot exceed 0.151 eV [44]. Because of this, we also calculate the lower bound mass value for the electron neutrino [33].

$$m_{\nu_e} \sim 1.4 \times 10^{-5} eV$$

$$\mu_{\nu_e}^0 = \frac{3eG_F m_{\nu_e}}{8\sqrt{2}\pi^2} = \frac{3m_e G_F m_{\nu_e}}{4\sqrt{2}\pi^2} (\mu_B) \approx 4.48 \times 10^{-24} \mu_B \quad [2.5.14]$$

We find this value to be slightly smaller than the value previously calculated by Schrock. This is because more precise constraints have been found for the mass of the electron neutrino in the early universe. We still see the same relationship where the mass of the neutrino is proportional to the magnetic moment.

Second Generation Lepton Flavor Muon (μ and ν_μ)

The value of the muon is currently a big research topic in physics because the experimental and theoretical calculations do not match. For the electron, the value that was found experimentally and theoretically was found to give the best approximation of the fine structure constant, α . The experimental values for the muon magnetic moment is currently 350 times worse than the value found for the electron. There are many experiments underway to create more sensitive instruments capable of enhancing the measurements [7, 44]. There is some speculation as to why this discrepancy is so large. The leading cause is supersymmetry.

At CERN in 1977, a series of experiments was done to determine the magnetic moment value for the muon. The experimental value found at CERN was,

$$a_\mu^{exp} = 116592300(840) \times 10^{-11} \quad [2.5.15]$$

A similar experiment was done years later in 1998 and 1999 at Brookhaven National Lab (BNL). Combining the results with CERN's results, they averaged the value for muon magnetic moment as:

$$a_{\mu}^{exp}(\text{Average}) = 116592023(151) \times 10^{-11} \quad [2.5.16]$$

The muon is more sensitive to radiative contributions by a factor of m^2 . This makes the experimental value better for calculations involving shorter distance phenomena. The experimental value requires a theoretical value as a comparison and the common problem is the theoretical value is not as reliable as scientists would like.

Czarnecki and Marciano [7] calculated the theoretical value for the muon magnetic moment. They used the same equation referenced in the electron section for QED radiative corrections:

$$a_{\mu}^{QED} = \frac{\alpha}{2\pi} + 0.765857376(27) \left(\frac{\alpha}{\pi}\right)^2 + 24.05050898(44) \left(\frac{\alpha}{\pi}\right)^3 + \dots$$

$$a_{\mu}^{QED} = 116584705.7(2.9) \times 10^{-11} \quad [2.5.17]$$

In this equation, the authors calculated the radiative corrections up to the 5th loop level [7]. They used the same value for the fine structure constant that was calculated from the electron magnetic moment value, $\alpha = \frac{1}{137}$.

The authors also show the calculations for the electroweak corrections to the muon magnetic moment. This equation calculated with the standard model in mind is,

$$a_{\mu}^{EW}(1 \text{ loop}) = \frac{5 G_F m_{\mu}^2}{3 8\sqrt{2}\pi^2} \times \left[1 + \frac{1}{5} (1 - 4 \sin^2 \theta_W)^2 + \mathcal{O}\left(\frac{m_{\mu}^2}{M_W^2}\right) \right]$$

$$\approx 195 \times 10^{-11} \quad [2.5.18]$$

G_F is the Fermi coupling constant and $\sin^2 \theta_W = 1 - \frac{M_W^2}{M_Z^2}$.

These one-loop diagrams are very similar to the diagrams previously shown for the electron. This is because they are both leptons that hold a charge. However, the muon has a larger mass than the electron and the individual lepton number conservation will be obeyed for L_μ instead of L_e .

The regular standard model value of the magnetic moment is in units of Bohr magneton given as:

$$a_\mu^{SM} = 116591597(67) \times 10^{-11} \quad [2.5.19]$$

Whereas the experimentally measured value of the magnetic moment of muon is found to be much higher than this. This measured value may not be due to only the electromagnetic interaction and may include the contribution of weak interactions as well. Combining the values found for QED, hadronic, and electroweak contributions give the value that is still almost 2.6 times higher than the measured value given as,

$$a_\mu^{exp} - a_\mu^{SM} = 426 \pm 165 \times 10^{-11} \quad [2.5.20]$$

Which is almost 158 % higher by than the calculated values and the difference is around 2.6×10^{-9} Bohr magneton. This means there is justification to find a correction to reconcile the results. This calculation will then give some new physics that is yet to be discovered. Supersymmetry is the most popular opinion and the chances of it being correct increase if the experimental value is validated. Supersymmetry would be an exciting solution to the magnetic moment discrepancies.

Muon Neutrino

Similar to their charged particle counterparts, the muon neutrino has similar properties to the electron neutrino, so we can use the same Feynman diagrams to explain the induced magnetic moment. In these diagrams, the difference is the muon is inducing the magnetic moment of the muon neutrino. These have different masses; and therefore, will show a different effect on the magnetic moment.

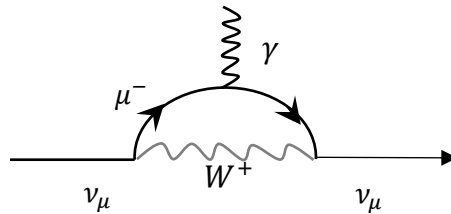


Figure [2.5.6]: Bubble diagram for muon neutrino in the minimal standard model.

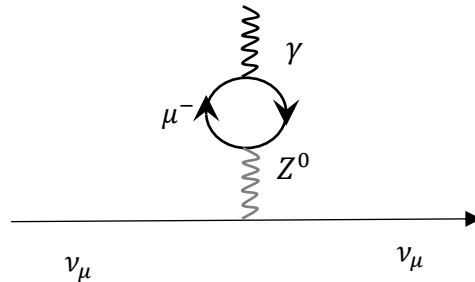


Figure [2.5.7]: Tadpole diagram for muon neutrino in the minimal standard model.

Similar to the electron neutrino, we use generalization of Schrock's equation:

$$\mu_{\nu_\ell}^0 = \frac{3eG_F m_{\nu_\ell}}{8\sqrt{2}\pi^2} = \frac{3m_e G_F m_{\nu_\ell}}{4\sqrt{2}\pi^2} (\mu_B) \approx 3.2 \times 10^{-19} \left(\frac{m_{\nu_\ell}}{1\text{eV}}\right) \mu_B \quad [2.5.21]$$

Next, we calculate the magnetic moment for the muon neutrino. The muon neutrino is affected by a muon which gives it an induced magnetic moment. The muon has a larger mass than the electron, which corresponds to the muon neutrino having a

larger magnetic moment than the electron neutrino. We will first use the upper bound mass found experimentally for the muon neutrino.

$$m_{\nu_\mu} \sim 1.9 \times 10^5 \text{ eV}$$

$$\mu_{\nu_\mu}^0 = \frac{3eG_F m_{\nu_\mu}}{8\sqrt{2}\pi^2} = \frac{3m_e G_F m_{\nu_\mu}}{4\sqrt{2}\pi^2} (\mu_B) \approx 6.08 \times 10^{-14} \mu_B \quad [2.5.22]$$

Using the lower bound mass value, we find the magnetic moment that is more likely to have occurred in the early universe. For this case, the added mass constraint of less than 0.151 eV is very important [33, 44].

$$m_{\nu_\mu} \sim 2.8 \times 10^{-3} \text{ eV}$$

$$\mu_{\nu_\mu}^0 = \frac{3eG_F m_{\nu_\mu}}{8\sqrt{2}\pi^2} = \frac{3m_e G_F m_{\nu_\mu}}{4\sqrt{2}\pi^2} (\mu_B) \approx 8.96 \times 10^{-22} \mu_B \quad [2.5.23]$$

This further proves the proportional relationship between mass and magnetic moment. It is interesting to see how big of a difference the magnetic moment is between the upper and lower bounds because of mass.

Third Generation Lepton Flavor Tau (τ and ν_τ)

The magnetic moment of tau is not directly measurable experimentally because the lifetime of the tau particle is very short. The particle is experimentally found through measurements of scattering of different reactions during specific energies. These will be examined more after the discussion of the theoretical calculations.

The authors, Eidelman and Passera, [9] review the theoretical approach to the tau magnetic moment. For $T=0$, the standard equation for fermion magnetic moment can be used.

$$\boldsymbol{\mu} = g \frac{e}{2m} \mathbf{s} \quad [2.5.24]$$

In this equation, $g=2$ and m and e represent the charge and mass of the particle. The spin is represented by s .

The authors calculate the QED radiative contributions for tau because of the importance of including the virtual particles that are continuously being absorbed and re-emitted. The value for the fine structure constant is found by using the masses of the other charged leptons.

$$\alpha_{\tau}^{QED} = A_1 \frac{\alpha}{2\pi} + A_2 \left(\frac{\alpha}{\pi}\right)^2 + A_3 \left(\frac{\alpha}{\pi}\right)^3 + \dots \quad [2.5.25]$$

Once the dimensionless constant is found, the authors use the following equation for up to three-loop corrections. For the tau particle, the authors found that higher order calculations are needed to be more precise.

$$\alpha_{\tau}^{QED} = A_i^{(2)} \frac{\alpha}{2\pi} + A_i^{(4)} \left(\frac{\alpha}{\pi}\right)^2 + A_i^{(6)} \left(\frac{\alpha}{\pi}\right)^3 + \dots \quad [2.5.26]$$

Adding up the calculations from different loop contributions equal the total value below for the QED contributions.

$$\alpha_{\tau}^{QED} = 117324(2) \times 10^{-8} \quad [2.5.27]$$

The electroweak contributions were required to get precise value for the tau magnetic moment in the theoretical standard model. The equation for the electroweak contributions for tau magnetic moment is below.

$$\begin{aligned} \alpha_{\tau}^{EW} (1 \text{ loop}) &= \frac{5G_F m_{\tau}^2}{24\sqrt{2}\pi^2} \times \left[1 + \frac{1}{5} (1 - 4 \sin^2 \theta_W)^2 + \mathcal{O}\left(\frac{m_{\tau}^2}{M_{W,Z,H}^2}\right) \right] \\ &\approx 55.1(1) \times 10^{-8} \end{aligned} \quad [2.5.28]$$

In the above equation, G_F is the Fermi coupling constant and M is the masses for the W, Z, and Higgs boson. θ_w is the value for the weak mixing angle.

These authors also included the hadronic contributions to calculate the tau magnetic moment. This accounts for the photon propagators and their self-energy.

$$a_\tau^{HAD} = a_\tau^{HLO} + a_\tau^{HHO}(vp) + a_\tau^{HHO}(lbl) = 350.1(4.8) \times 10^{-8} \quad [2.5.29]$$

The total magnetic moment for the standard model is found by adding up the contributions stated above.

$$a_\tau^{SM} = 117721(5) \times 10^{-8} \quad [2.5.30]$$

The measurements of tau magnetic moment are more difficult to find because the tau particle decays faster than other leptons. To measure this value, the tau decay products must be included. In the DELPHI experiment, the tau magnetic moment was measured from the scattering during $e^+e^- \rightarrow e^+e^-\tau^+\tau^-$ decay. Measuring the cross section resulted in the answer below.

$$a_\tau = 0.018 \pm 0.017 \quad [2.5.31]$$

When we compare the results of theoretical calculation and experimental value, we see there is a discrepancy. Similar to the muon, this could mean new physics to be discovered. A lot of information is known about the electroweak contributions, but the tau particle still has a lot of unknowns.

The vacuum values of all charged leptons are located in Table [5.1.1] and are shown in units of Bohr magneton for comparison.

Tau Neutrino

We use the same Feynman diagrams as the other neutrino flavors, but use the corresponding charged lepton, tau. This neutrino is the heaviest and most elusive.

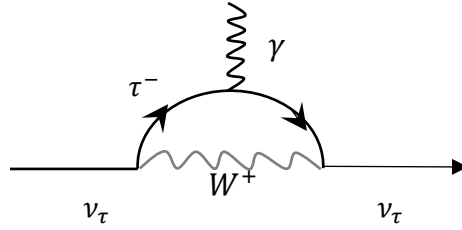


Figure [2.5.8]: Bubble diagram for tau neutrino in the minimal standard model.

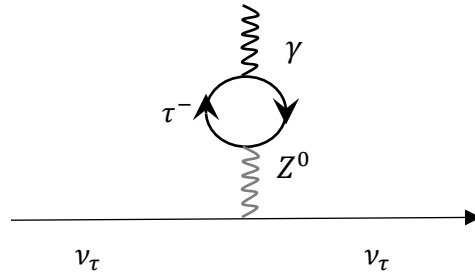


Figure [2.5.9]: Tadpole diagram for tau neutrino in the minimal standard model.

Once again, we use the generalization of Schrock's calculation below:

$$\mu_{\nu_\ell}^0 = \frac{3eG_F m_{\nu_\ell}}{8\sqrt{2}\pi^2} = \frac{3m_e G_F m_{\nu_\ell}}{4\sqrt{2}\pi^2} (\mu_B) \approx 3.2 \times 10^{-19} \left(\frac{m_{\nu_\ell}}{1\text{eV}}\right) \mu_B \quad [2.5.32]$$

The last type of neutrino is the tau neutrino. The mass of this neutrino is the largest of all the neutrinos similar to the tau particles which have the heaviest mass among leptons. The upper most bound on tau neutrino was found experimentally and recorded by the Particle Data Library [44]. We use this to find the vacuum value of magnetic moment.

$$m_{\nu_\tau} \sim 1.82 \times 10^7 eV$$

$$\mu_{\nu_\tau}^0 = \frac{3eG_F m_{\nu_\tau}}{8\sqrt{2}\pi^2} = \frac{3m_e G_F m_{\nu_\tau}}{4\sqrt{2}\pi^2} (\mu_B) \approx 5.83 \times 10^{-12} \mu_B \quad [2.5.33]$$

This value is much too large for early universe calculations. The sum of all neutrino mass eigenstates cannot exceed a mass of 0.151 eV [44]. We also calculate the lower bound mass value for the tau neutrino [33].

$$m_{\nu_\tau} \sim 4.8 \times 10^{-2} eV$$

$$\mu_{\nu_\tau}^0 = \frac{3eG_F m_{\nu_\tau}}{8\sqrt{2}\pi^2} = \frac{3m_e G_F m_{\nu_\tau}}{4\sqrt{2}\pi^2} (\mu_B) \approx 1.54 \times 10^{-20} \mu_B \quad [2.5.34]$$

The tau neutrino is affected by the tau particle in the largest way compared to the other neutrino flavors. Because this is the largest particle, the effect of the magnetic moment on the particle is larger.

CHAPTER III:

MAGNETIC MOMENT OF LEPTONS IN HIGH TEMPERATURE

Intrinsic magnetic moment of a particle changes due to a change in mass in the medium [21-23]. Masood [34] has calculated the self-mass and magnetic moment of an electron in hot and dense media for different regions of temperature and chemical potential. The renormalized mass of a lepton starts out as,

$$m_\ell^{phys} = m_\ell + \delta m_\ell \quad [3.0.1]$$

This is equal to one-loop level as discussed earlier in the section and matches the values of electron self-mass. The variable m_ℓ represents the mass of the charged lepton with no temperature or radiative corrections included. The calculation for up to the second loop level, α^2 , equals the equation below.

$$m_{\ell_{phys}} \sim = m_\ell + \delta m_\ell^{(1)} + \delta m_\ell^{(2)} \quad [3.0.2]$$

We will not be using the second-loop level in this thesis, but this equation is important to understand the relationship between mass and multiple loop levels. Next, we need to include the boson and fermion temperature dependent propagators and calculate their loop integrals to find the corrections. The first order temperature correction for the electron mass at finite temperature is equal to:

$$\begin{aligned} \frac{\delta m_\ell}{m_\ell} &\simeq \frac{1}{2m_\ell^2} \{(m_\ell^{phys})^2 - m_\ell^2\} \\ &\simeq \frac{\alpha\pi T^2}{3m_\ell} \left[1 - \frac{6}{\pi^2} c(m_\ell\beta) \right] + \frac{2\alpha}{\pi} \frac{T}{m_\ell} a(m_\ell\beta) - \frac{3\alpha}{\pi} b(m_\ell\beta) \end{aligned} \quad [3.0.3]$$

The coefficients of a, b, and c all react differently to different temperatures. At low temperatures these coefficients are minimal and can be dropped off, as shown below:

$$\frac{\delta m_\ell}{m_\ell} \xrightarrow{T \ll m_\ell} \frac{\alpha \pi T^2}{3 m_\ell^2} \quad [3.0.4]$$

The calculation at a higher temperature is slightly different. The coefficients a and b are very small and vanish, so that c is all that contributes. The value of c becomes $c = -\frac{\pi^2}{12}$ in this limit, giving

$$\frac{\delta m_\ell}{m_\ell} \xrightarrow{T \gg m_\ell} \frac{\alpha \pi T^2}{2 m_\ell^2} \quad [3.0.5]$$

Equation [3.0.3] can be used in calculations pertaining to primordial nucleosynthesis and early universe and the other equations can be used in calculations for other magnetic moments. This is because the electron is a charged particle that effects the magnetic moment of other particles. These equations are also relevant in neutron and proton magnetic moment because the electron magnetic moment effects the magnetic moment of various particles that are not charged.

First Generation Lepton Flavor Electron (e and ν_e)

Electron

The radiative corrections to the electron self-mass from the surrounding thermal background of fermions and bosons are very important to the magnetic moment calculations. This is shown by calculating the one-loop level corrections and applying it to the electron's magnetic moment. The contribution of two-loop on the magnetic moment of the electron has also been calculated, but for the purpose of this thesis we only calculate up to one-loop level. It has been shown that the contribution of one-loop is significant compared to the contribution of two-loop. The electron interacts with external

magnetic fields through its mass. This interaction at a finite temperature is seen in the equation below:

$$\mu_a = \frac{\alpha}{2\pi} - \frac{2}{3} \frac{\delta m_\ell}{m_\ell} \quad [3.1.1]$$

The above calculation is applied to the one-loop corrections to the magnetic moment equation which included the coefficients a, b, and c [3].

$$\mu_a = \frac{\alpha}{2\pi} - \frac{2}{3} \alpha \left[\frac{\pi T^2}{3m_\ell^2} \left\{ 1 - \frac{6}{\pi} c(m_\ell \beta) \right\} + \frac{2}{\pi} \frac{T}{m_\ell} a(m_\ell \beta) - b(m_\ell \beta) \right] \quad [3.1.2]$$

This equation shows what the magnetic moment would be for an instance in time where $T \sim m$. This temperature is present in primordial nucleosynthesis, which is not long after the Big Bang. Once simplified, the equation for the magnetic moment of charged leptons in $T \ll m_\ell$, becomes:

$$\mu_a = \frac{\alpha}{2\pi} - \frac{2}{9} \frac{\alpha \pi T^2}{m_\ell^2} \quad [3.1.3]$$

At very low temperatures such as this, fermions stop contributing and only photons are incorporated in the hot thermal background. Self-interacting photons are not included in α because of their absence in QED. Nucleosynthesis took place in the universe when $T > m_e$ [22], and we mainly consider nucleosynthesis temperatures for this calculation. Magnetic moment for charged leptons can then be expressed as:

$$\mu_a = \frac{\alpha}{2\pi} - \frac{1}{3} \frac{\alpha \pi T^2}{m_\ell^2}, \quad [3.1.4]$$

Whereas the fine structure constant is given as:

$$\alpha = \frac{e^2}{4\pi\hbar c} \approx \frac{1}{137} \quad [3.1.5]$$

The next step is changing the mass into units of temperature, given in Kelvin. For this we use the equation that relates energy to temperature.

$$m_e c^2 = k_B T \quad [3.1.6]$$

where, k_B is the Boltzmann constant. We use the relation: $c = \hbar = k_B = 1$. The temperature value in terms of electron Volts then becomes,

$$m_e \approx T \approx 0.511 \times 10^6 eV \quad [3.1.7]$$

Thermal contributions to the magnetic moment of electron before nucleosynthesis [22] at $T \gg m_e$ is:

$$\mu_e = 1.17 \times 10^{-3} \left(1 - \frac{\pi^2 T^2}{3m_e^2} \right) \mu_B \quad [3.1.8]$$

Whereas, for $T \ll m_e$, the magnetic moment value comes out to be:

$$\mu_e = 1.17 \times 10^{-3} \left(1 - \frac{2\pi^2 T^2}{9m_e^2} \right) \quad [3.1.9]$$

This value is negative because this calculation is for charged particles. For particles that are not charged, the value is positive. We see this value is much larger than the value of the magnetic moment in a vacuum. This is because the electron couples with the surrounding magnetic field and gains mass. The thermal contribution of charged particles is inversely proportional, so the electron has the greatest thermal contribution and magnetic moment. The high temperature thermal contribution is greater than the vacuum value for magnetic moment, which causes a flip in the electron magnetic moment.

Electron Neutrino

The electron type Dirac neutrino interacts with charged electron only to gain an induced magnetic moment. Dirac neutrinos can interact with the medium and therefore, there is an increasingly proportional relationship between the magnetic moment of the particle and the temperature. To start, the boson and fermion propagators need to be calculated [31]. These are the propagators in the surrounding area that could have an effect on the neutrino. The boson propagator is important because it helps calculate the probability that a boson will travel in a region from one place to another and effect the neutrino's magnetic moment. To obtain this calculation, Green's function of the Schrodinger equation is used. The equation is shown below:

$$D_B^\beta = \frac{1}{k^2 + i\varepsilon} - 2\pi i \delta(k^2) n_B(k) \quad [3.1.10]$$

$$n_B(k) = \frac{1}{e^{\beta k_0} - 1} \quad [3.1.11]$$

The fermion propagator is similar to the boson propagator, but it calculates the likelihood of a fermion interacting in a specific region and time with the neutrino. This equation is shown below:

$$S_F^\beta = (p - m_l) \left[\frac{1}{p^2 - m_l^2 + i\varepsilon} + 2\pi i \delta(p^2 - m_l^2) n_F(p) \right] \quad [3.1.12]$$

$$n_F(p) = \frac{\theta(p_0)}{e^{\beta(p_0 - \mu)} + 1} + \frac{\theta(-p_0)}{e^{\beta(p_0 + \mu)} + 1} \quad [3.1.13]$$

In the above equation, $n_F(p)$ correspond to Fermi-Dirac distribution. This shows that the fermions and anti-fermions have an equal and opposite chemical potential to one another. This is in a CP symmetric background where the number of particles and anti-particles are equal.

In this thesis, we use the previously calculated results by Masood [31] and others for the basic form factors of a neutrino to incorporate their contributions to leptonic decays including Plasmon decay. Plasmon is the quantization of plasma oscillations of electron gas. When it decays, it gives off both a neutrino and an antineutrino. From this decay, we can calculate the electromagnetic form factors of the Dirac neutrino. This equation can be seen below:

$$\Gamma_\mu = [F_1 \bar{g}_{\mu\nu} \gamma^\nu + F_2 u_\mu + iF_3 (\gamma_\mu u_\nu - \gamma_\nu u_\mu) q^\nu + iF_4 \varepsilon_{\mu\nu\alpha\beta} \gamma^\nu q^\alpha u^\beta] L \quad [3.1.14]$$

Where,

$$F_1 = T_T + \frac{\omega}{Q^2} (T_L - T_T) \quad [3.1.15.a]$$

$$F_2 = \frac{1}{v^2} (T_L - T_T) \quad [3.1.15.b]$$

$$iF_3 = -\frac{\omega}{Q^2} (T_L - T_T) \quad [3.1.15.c]$$

$$F_4 = \frac{T_P}{Q} \quad [3.1.15.d]$$

Here, F_1 is the charge radius, F_2 is the magnetic dipole moment, F_3 is the electric dipole moment, and F_4 is the anapole moment. These equations use the Transverse (T_T), Longitudinal (T_L), and Polarization (T_P) components of the vertex equation to describe the direction of propagation.

$$T_T = \frac{eg^2}{2M^2} \left(\alpha - \frac{\beta}{u^2} \right) \quad [3.1.16.a]$$

$$T_L = \frac{eg^2}{M^2} \frac{\beta}{u^2} \quad [3.1.16.b]$$

$$T_P = -\frac{eg^2}{M^2} |q|\kappa \quad [3.1.16.c]$$

In the above equations, α , β , and κ correspond to the below integrals:

$$\alpha = \int \frac{d^3p}{(2\pi)^{3/2E}} (n_F^+ + n_F^-) \left[\frac{2m^2 - 2p \cdot q}{q^2 + 2p \cdot q} + (q \leftrightarrow -q) \right] \quad [3.1.17.a]$$

$$\beta = \int \frac{d^3p}{(2\pi)^{3/2E}} (n_F^+ + n_F^-) \left[\frac{2(p \cdot u)^2 - 2(p \cdot u)(q \cdot u) - p \cdot q}{q^2 - 2p \cdot q} + (q \leftrightarrow -q) \right] \quad [3.1.17.b]$$

$$\kappa = - \int \frac{d^3 p}{(2\pi)^{32E}} (n_F^+ - n_F^-) \left[\frac{1}{q^2 + 2p \cdot q} + (q \leftrightarrow -q) \right] \quad [3.1.17.c]$$

Depending on the type of medium, these integrals give different results that effect the electromagnetic form factors. At $T \geq \mu$:

$$\alpha \simeq \frac{1}{\pi^2} \left[\frac{c(m_\ell \beta, \mu)}{\beta^2} + \frac{m}{\beta} a(m_\ell \beta, \mu) - \frac{m^2}{2} b(m_\ell \beta, \mu) - \frac{m^4 \beta^2}{8} h(m_\ell \beta, \mu) \right] \quad [3.1.18.a]$$

$$\beta \simeq \frac{1}{\pi^2} \left[\left(1 + \frac{3}{8} \ln \frac{1-v}{1+v}\right) \frac{c(m_\ell \beta, \mu)}{\beta^2} + \frac{m}{\beta} a(m_\ell \beta, \mu) - \frac{m^2}{2} b(m_\ell \beta, \mu) - \frac{m^4 \beta^2}{8} h(m_\ell \beta, \mu) \right] \quad [3.1.18.b]$$

$$\kappa \simeq \frac{1}{\pi^2} [b(m_\ell \beta, \mu) + m_\ell^2 h(m_\ell \beta, \mu)] \quad [3.1.18.c]$$

The vertex function for the neutrino during Plasmon decay using the case of the bubble diagram in Chapter II is shown below:

$$\begin{aligned} \Lambda_0(p_1, p_2) = & - \frac{g^2}{m_w^2} \int \frac{d^4 k}{(2\pi)^4} \gamma_\alpha L(p_2 - k + m_l) \gamma_\mu (p_1 - k + \\ & m_l) \gamma^\alpha L \frac{2\pi i \delta[(p_2 - k)^2 - m_l^2]}{(p_2 - k)^2 - m_l^2} n_F(p_2 - k) + (p_1 \leftrightarrow p_2) \end{aligned} \quad [3.1.19]$$

From this vertex equation we calculate the magnetic moment contribution for massive neutrinos in high temperature. In this case, $k \rightarrow 0$ as chemical potential approaches zero.

$$\alpha_v^\beta \approx \frac{G_F m_l}{4\pi^2} m_{\nu_l} \left[b(m \beta) + \frac{4}{M^2} (m a(m \beta) - c(m \beta)) \right] \mu_B \quad [3.1.20]$$

Setting: $c(m \beta) = -\frac{\pi^2}{12}$ cancels out the $4\pi^2$, and leaves us with the general equation for the thermal contribution on magnetic moment of all neutrino flavors:

$$a_{\nu_\ell} = \frac{T^2 G_F m_e m_{\nu_\ell}}{12M^2} \mu_B \quad [3.1.21]$$

This is the major contribution from the bubble diagrams in Chapter II. In order to use the same units and relations as the charged leptons to compare the magnetic moment, we need to use the following relation:

$$\left(\frac{T}{m_e}\right)^2 = 1 \quad [3.1.22]$$

This is necessary because the neutrino calculations do not have the electron mass in the denominator, so we must add it to convert the temperature from Kelvin into electron Volts. We use the specific masses for both the upper mass bound and lower mass bound of neutrinos [33, 38, 44] to find how thermal contributions effect the magnetic moment. The upper and lower bounds for mass were found experimentally. The lower bounds have the possibility of corresponding with mass used in cosmology models. This is because in the early universe the neutrino mass had to be below the neutrino decoupling temperature.

Upper mass bound gives:

$$a_{\nu_e}^u = \frac{T^2 G_F m_e m_{\nu_e}}{12M^2} \mu_B \approx 6.58 \times 10^{-16} \mu_B \quad [3.1.23.a]$$

Lower mass bound gives:

$$a_{\nu_e}^L = \frac{T^2 G_F m_e m_{\nu_e}}{12M^2} \mu_B \approx 4.12 \times 10^{-21} \mu_B \quad [3.1.23.b]$$

Second Generation Lepton Flavor Muon (μ and ν_μ)

Muon

Because all the muons have similar properties to that of electrons, we can use the same equation to calculate the magnetic moment in hot media. The difference is that the photons interact through muon loops because of flavor conservation. We do show in Table [5.1.1] that the corresponding temperature for each individual lepton mass will be with the different lepton flavors. For comparison purposes we use the temperature of primordial nucleosynthesis in our calculations for the muon and tau. This temperature comes out to be approximately equal to the electron mass.

$$T \approx 0.511 \times 10^6 eV \quad [3.2.1]$$

We use the calculation for $T \ll m_\ell$ because the mass of an electron is smaller than the mass of the muon.

$$\mu_a = \frac{\alpha}{2\pi} - \frac{2\alpha\pi T^2}{9m_\ell^2} \quad [3.2.2]$$

This calculation simplifies to:

$$\mu_\mu = 1.17 \times 10^{-3} \left(1 - \frac{2\pi T^2}{3m_\mu^2} \right) \mu_B \quad [3.2.3]$$

We can simplify this even further because subtracting such a small number from 1 does not give us the significance we need. Because of this, we do not subtract from 1 and the calculation becomes:

$$\mu_\mu = - \left(\frac{2\pi\alpha T^2}{9m_\mu^2} \right) \mu_B = -1.19 \times 10^{-7} \mu_B \quad [3.2.4]$$

We notice this value is opposite in sign, which corresponds to our same reasoning for the electron because they are charged leptons. This value for magnetic moment is smaller because the mass of the muon is larger than the electron and the temperature is inversely proportional to mass.

Muon Neutrino

We consider all the flavors of neutrinos which have similar contributions (except for mass), when we calculate the magnetic moment at high temperature. We use the bubble diagram that corresponds to the muon neutrino for calculating the vertex function found from the Plasmon decay form factors with the electron neutrino:

$$\Lambda_0(p_1, p_2) = -\frac{g^2}{m_w^2} \int \frac{d^4 k}{(2\pi)^4} \gamma_\alpha L(p_2 - k + m_l) \gamma_\mu (p_1 - k + m_l) \gamma^\alpha L \frac{2\pi i \delta[(p_2 - k)^2 - m_l^2]}{(p_2 - k)^2 - m_l^2} n_F(p_2 - k) + (p_1 \leftrightarrow p_2) \quad [3.2.5]$$

We set $k \rightarrow 0$ because the chemical potential approaches zero and find the magnetic moment equation for thermal contribution for all neutrino flavors:

$$a_{\nu_\ell} = \frac{T^2 G_F m_e m_{\nu_\ell}}{12M^2} \mu_B \quad [3.2.6]$$

Inputting the specific masses for the muon neutrino for both the upper bound and lower bound mass [33, 44], we find the thermal contributions effect on the muon neutrino magnetic moment.

Upper bounds:

$$a_{\nu_\mu}^u = \frac{T^2 G_F m_e m_{\nu_\mu}}{12M^2} \mu_B \approx 5.55 \times 10^{-11} \mu_B \quad [3.2.7.a]$$

Lower bounds:

$$a_{\nu_\mu}^L = \frac{T^2 G_F m_e m_{\nu_\mu}}{12M^2} \mu_B \approx 8.24 \times 10^{-19} \mu_B \quad [3.2.7.b]$$

Third Generation Lepton Flavor Tau (τ and ν_τ)

Tau

Using the same calculations as the electron and muon particles, we continue the magnetic moment calculations for the tauon. In this case, photons interact through tau loops. Using the same temperature that is equivalent to electron mass:

$$T \approx 0.511 \times 10^6 eV \quad [3.3.1]$$

We use the same calculation as muon for $T \ll m_\ell$ because the mass of an electron is even smaller than the mass of the tauon.

$$\mu_\alpha = \frac{\alpha}{2\pi} - \frac{2}{9} \frac{\alpha\pi T^2}{m_\ell^2} \quad [3.3.2]$$

Simplifying the calculation in a similar way as the muon particle equals:

$$\mu_\tau = - \left(\frac{2\pi\alpha T^2}{9m_\tau^2} \right) \mu_B = -4.2 \times 10^{-11} \mu_B \quad [3.3.3]$$

The temperature contribution is much smaller for the tauon because the more mass is added to the particle, the more difficult it is to torque.

Tau Neutrino

We use the same equations as the other two neutrino flavors [31] to calculate the thermal contribution effects on magnetic moment for tau neutrino. The following generalized equation is used:

$$a_{\nu_\ell} = \frac{T^2 G_F m_e m_{\nu_\ell}}{12M^2} \mu_B \quad [3.3.4]$$

Using the upper and lower bound masses for the tau neutrino leads us to the thermal contribution effect on the tau neutrino magnetic moment.

Upper bound:

$$a_{\nu_\tau}^u = \frac{T^2 G_F m_e m_{\nu_\tau}}{12M^2} \mu_B \approx 4.53 \times 10^{-9} \mu_B \quad [3.3.5.a]$$

Lower bound:

$$a_{\nu_\tau}^L = \frac{T^2 G_F m_e m_{\nu_\tau}}{12M^2} \mu_B \approx 1.41 \times 10^{-17} \mu_B \quad [3.3.5.b]$$

With these results, we can see that the contribution of thermal effects in terms of mass, so the heaviest neutrinos will have the greatest magnetic moment. In these calculations we do not include temperature in the charge or coupling constant. This is because in QED these changes in value are not significant enough to greatly affect the results when we are comparing mass and magnetic moment and will be suppressed by the QED coupling constants.

Majorana Neutrinos

The term Majorana, when used in particle physics refers to the particle being its own anti-particle. Massive Majorana neutrinos are similar to Dirac neutrinos with spin $\frac{1}{2}$. The main difference between the two is that Dirac particles have four degrees of freedom and Majorana only have two. This is because the Majorana particles are also anti-particles of themselves. The Majorana neutrino cannot have a magnetic or electric dipole moment like the Dirac neutrino. This is because they have different electromagnetic properties [4]. This can be seen from the following form factors of the antineutrino.

$$\bar{f}_\Omega^{ft} = -f_\Omega^{ft} \quad (\Omega = Q, M, E) \quad [3.4.1]$$

$$\bar{f}_A^{ft} = f_A^{ft} \quad [3.4.2]$$

The electromagnetic form factors for the Dirac neutrino that show the neutrino and antineutrino are not equal and cannot exist in the Majorana neutrinos. These three form factors are the charge radius, magnetic dipole moment, and electric dipole moment. All of these are symmetric for Dirac neutrinos, which means they are imaginary for Majorana neutrinos. This is different for the anapole moment. For Dirac neutrinos the anapole moment is antisymmetric and imaginary; but for Majorana neutrinos, anapole moment is the only real form factor.

The Majorana particle can have a magnetic and electric dipole moment when considering two neutrinos. This is because the Majorana neutrino will mix and change into a different flavor of neutrino between its initial and final state [4]. It has been calculated that the Majorana neutrino transition magnetic moment values are very similar to the values for the Dirac neutrino cases [33] and differ by an integral factor only. The neutrinos in SUSY (Supersymmetry) models can only have transition magnetic moments [33], which is very interesting because they would have to be Majorana neutrinos. However, SUSY allows for the integration of contributions from many more diagrams as the couplings are totally different from QED only.

Riotto [41] calculated the vertex equation with various models for the electron filled background where charged particles coupled with neutrinos. He found that Majorana magnetic and electric dipole moments in this medium are not significant. In this medium, a new value flips the chirality of the particle when adding the vertex function of the Dirac neutrino and antineutrino together.

$$\begin{aligned}
\Gamma_{\mu}^{L,R,Majorana}(p_1, p_2, u) \\
= \Gamma_{\mu}^{L,R,Dirac}(p_1, p_2, u) + \eta_e \eta_{\mu} \gamma^0 [C \Gamma_{\mu}^{L,R,Dirac}(-p_1, -p_2, u) C^{-1}]^* \gamma^0
\end{aligned}
\tag{3.4.3}$$

The electromagnetic vertex function with the added chirality flipping operators becomes:

$$\Gamma_{\mu}^{L,R,Majorana} = \left[F_1 \widetilde{u}_{\mu} (L + \eta_e \eta_{\mu} R) + i \frac{F_2}{2} (1 - \eta_e \eta_{\mu}) \sigma_{\mu\nu} q^{\nu} + i \frac{F_2}{2} \sigma_{\mu\nu} \gamma_5 (1 + \eta_e \eta_{\mu}) q^{\nu} \right] \quad [3.4.4]$$

In this equation, $R = \frac{(1+\gamma_5)}{2}$ is the chirality operator for right-handedness. We calculate these with q as the total momenta instead of p_1 and p_2 , individually. F_1 represents the chirality contribution and F_2 represents the contribution from both the electric and magnetic moments in the medium. This adheres to the limit of $q^2 = 0$ because k and q are 4-momenta vectors. The equations for both are given below.

$$F_1 = e \frac{\lambda_{123} \lambda_{131}}{2} \sin 2\theta_3 \left[\frac{1}{m_{23}^2} - \frac{1}{m_{13}^2} \right] m_e 2q^2 \times \int \frac{d^3k}{(2\pi)^2} \frac{(f_- - f_+)}{2E} \frac{(u \cdot k)}{(q^2 + 2k \cdot q)(q^2 - 2k \cdot q)} \quad [3.4.5]$$

$$F_2 = e \frac{\lambda_{123} \lambda_{131}}{2} \sin 2\theta_3 \left[\frac{1}{m_{23}^2} - \frac{1}{m_{13}^2} \right] m_e 2q^2 \times \int \frac{d^3k}{(2\pi)^2} \frac{(f_- + f_+)}{2E} \frac{1}{(q^2 + 2k \cdot q)(q^2 - 2k \cdot q)} \quad [3.4.6]$$

These calculations only work if the background has broken charge, parity, and time reversal (CPT) symmetry. It is only allowed to be broken in the background because all Lorentz invariant quantum field theories must be CPT symmetric. Identifying if the neutrino has transition or diagonal magnetic moments is one popular way to tell if a neutrino is a Majorana neutrino vs a Dirac neutrino because of these different electromagnetic properties [41].

Weyl Massless Neutrino

The massless neutrino has a magnetic moment of zero. Weyl or massless neutrinos cannot couple with magnetic fields on their own, even if they are very strong. This is because effective mass is increasingly proportional to the strength of a magnetic field. Weyl neutrinos are not able to directly interact with the medium they reside in, but they can interact and gain mass from a high density of electrons [31].

With this newly gained effective mass, Weyl neutrinos behave similar to Dirac neutrinos and can be calculated similarly. The below equation shows the relationship between effective mass, a constant magnetic field, and the chemical potential.

$$m_{eff} = \frac{g^2 e|B|\mu_e}{(2\pi^2)(m_W^2 - e|B|)} = \frac{g^2 \mu_e eB/m_W^2}{(2\pi^2)(1 - eB/m_W^2)} \quad [3.5.1]$$

In these equations, B is the magnetic field, g is the coupling constant, m_W is the mass of the W boson, and μ_e corresponds to the chemical potential of the density of electrons. The chemical potential also plays an important role in effective mass; and therefore, magnetic moment. The relationship between chemical potential and effective mass is similar to the relationship between the magnetic field and effective mass. The more chemical potential a particle has, the larger effective mass it will have. This density of electrons along with a very high magnetic field are only possible in superdense star systems.

The effective mass of the neutrino and the magnetic field couple together. The relationship can be seen below when taking the rate of change between the two. There is no background correction calculated because temperature has no effect on effective magnetic moment.

$$\frac{dm_{eff}}{dB} = \frac{g^2 e \mu_e}{(2\pi)^2 (m_W^2 - eB)} \left(1 + \frac{eB}{(m_W^2 - eB)} \right) \quad [3.5.2]$$

In these equations, the mass of the W boson acts as a ceiling for the total mass that can be acquired from the magnetic field. This can be seen through this equation: $e|B| \ll m_W^2$. Adding in this limit of a very small magnetic field creates this equation below.

$$\frac{dm_{eff}}{dB} = \frac{g^2 e \mu_e}{(2\pi)^2 m_W^2} \left(1 + \frac{eB}{m_W^2}\right) \approx \frac{g^2 e \mu_e}{(2\pi)^2 m_W^2} \quad [3.5.3]$$

When taking the opposite of that limit and instead finding the equation for a very large magnetic field, replace m_W^2 with $e|B|$ and it becomes:

$$\frac{dm_{eff}}{dB} = \frac{g^2 e \mu_e}{(2\pi)^2 eB} \quad [3.5.4]$$

From [3.5.3], we can see that when the magnetic field is very small, it is not included in the equation at all. We only factor in the mass for the W boson. With a very large magnetic field, the value for the magnetic moment will be large as long as the chemical potential is also large. The equation for a very large chemical potential and very large magnetic field is below. The magnetic field would have to be millions of Tesla to be large enough to make a difference in the magnetic moment. This equates to neutrons stars, especially magnetars. Magnetars are a type of neutron stars that have very strong magnetic fields. Their magnetic field strength can be $10^8 - 10^{11}$ Tesla [5]. For reference, the Earth's magnetic field is roughly 50 micro Tesla. Equation [3.5.2] then becomes the below equation for the magnetic moment of a Weyl neutrino.

$$\frac{dm_{eff}}{dB} = \frac{g^2 e \mu_e m_W^2}{(2\pi)^2 (m_W^2 - e|B|)^2} \quad [3.5.5]$$

The combination of these two create what is called the effective magnetic moment.

$$(\alpha_{\nu_l}^B)_{eff} \equiv \frac{dm_{eff}}{dB} \quad [3.5.6]$$

This is helpful in solving early universe problems as well as the Solar Neutrino Problem. It is most useful in situations when lepton scattering is being calculated.

CHAPTER IV: DISCUSSION

Our calculations show the importance of perturbation theory of quantum mechanics and how it helps to understand the basic concept of magnetic moment. It shows that the neutral particles may have a nonzero magnetic moment as a perturbative effect. QED is also very important and is considered the simplest gauge theory in explaining the interactions between light and matter. It incorporates thermal medium effects through the vacuum fluctuations of particle propagators as well as background particles that are floating in the heat bath. Perturbation theory of QED plays a vital role in our calculations for the magnetic moment at finite temperature.

Our calculations also include the existence of the sterile neutrino. This is because observations of solar and atmospheric neutrinos have been discovered to be inconsistent and require the existence of the sterile neutrino. The sterile neutrino is present as the right-handed component. This is because we are using the left-handed electroweak theory of the original standard model and adding mass to the neutrinos [31, 33]. We know that the mass of neutrinos has been measured experimentally and the electroweak theory has been tested experimentally. We use electroweak theory with massive neutrinos to understand the effects of mass and magnetic moment of neutrinos.

It is very important to calculate the magnetic moment of all neutrinos in high temperatures. Heavier particles were more present in the early universe; and therefore, are more important to consider. This means that tau and muon particles were more abundant than electrons. This also applies to the corresponding neutrinos. These calculations go from one particle systems that are used in vacuum calculations to many body systems that are used in high temperature calculations. This is because the statistical background in this environment was full of particles being created and annihilated.

The implications of the magnetic moment of leptons is significant in the early universe. For these calculations, the most accurate known model should be referenced. This is the cosmology limit on neutrino mass that states the sum of all the neutrino mass eigenstates are less than 0.151 eV [6, 44]. This corresponds to the lower bound neutrino masses. These calculations show that the contributions from the surrounding hot particles are significant and does have an effect on the magnetic moment of leptons.

These applications are significant in cosmology. The cosmology reference has been mentioned above when $T \sim m$ and where primordial nucleosynthesis occurred. During this time, a hot plasma full of electrons and photons filled the universe. It was too hot for atoms to form for a long time, so this time is very important.

Another significant application for these calculations is in astrophysics [10-12]. High mass stars have enough gravitational energy that when they exhaust their Helium fuel, their temperatures become very hot. Also, the cores of neutron stars are filled with very dense plasmas and emit large amounts of neutrinos [5]. During these cases with hot plasmas and particle emission, we can find how the hot surrounding media effects the magnetic moment of the particles; and in turn, what this means for the surrounding universe.

Beta decay is a nuclear process where an electron and neutrino are emitted from a nucleus. This occurs because a neutron is changing into a proton or vice versa. Beta decay is very common in the universe. It is known to occur in stellar cores, hot and dense medium, as well as here on Earth. Beta decay is a weak process that plays a large role in primordial nucleosynthesis. When temperatures cool down to 10^{10} K and baryon densities drop to 10^{-10} K, the beta decay process can start. It is known that the mass of the particles and the medium conditions effect rate of beta decay.

Studying the beta decay process helps to better understand nucleosynthesis [26]. Because electrons are important components of beta decay, these electromagnetic property changes must be calculated in different media in order to fully understand beta decay and the electron.

It has been shown that the thermal contributions from the background media contribute directly to beta decay [26]. This is because the thermal contribution of the electron self-mass can be inserted directly into the equation to describe how radiative corrections relate to beta decay. This is best studied at higher loop levels because the contributions to beta decay vary in terms of the temperature.

The first major particles that were produced in the early universe were leptons. This gives more reason to study these particles in detail because they are linked to many unsolved mysteries in our universe. It is known that through vacuum polarization in QED plasma, the lepton mass and charge are modified [27-33]. Based on this, we know that the magnetic moment of leptons in high temperatures will have relevant implications to this process in the early universe.

Neutrinos are known to have an effect on both the weak interaction and expansion rates of the early universe [11]. This is because neutrino decoupling happens when the universe starts to cool down ($T \sim m_e$), which corresponds to the neutron/proton freeze out ratio during nucleosynthesis. Knowing the exact values of the magnetic moment of neutrinos during this time could help calculations for the abundance of particles created at that time. The neutrinos effect on this ratio influences the number of light nuclei produced because of its effect on the weak interaction rates during these processes. The weak interaction rates are responsible for the equilibrium between protons and neutrons during nucleosynthesis. This proves to be a relevant calculation in big bang nucleosynthesis.

The magnetic moment of charged leptons is inversely proportional to the mass of the particle. This means that heavier particles have a smaller magnetic moment than lighter ones. This is the opposite for neutrinos. Neutrino magnetic moment is proportional to the mass. This means that the tau neutrino flavor has a greater magnetic moment than the electron neutrino. This also means that the thermal contributions to the neutrinos contribute more significantly to the heavy tau neutrino than the lighter electron neutrino at nucleosynthesis temperatures. It should be noted that the existence of heavier neutrinos will be significant at only higher energies.

We have subtracted the thermal contribution from the vacuum value of magnetic moment, which reduces its total value when the temperature increases. Our calculations show that the magnetic moment for the electron is affected most by thermal contributions. This contribution is around 0.7% and can be seen in Table [5.1.1]. The thermal contributions to the muon and tau particles are smaller and ignorable. When the temperature reaches a much higher value closer to the mass of the tau particle, the magnetic moment will no longer be ignorable. Figures [5.1.1.a,b,c] below are graphs plotting the magnetic moment of each charged lepton flavor as a function of temperature. The magnetic moment is in units of Bohr magneton for comparison purposes.

Figure [5.1.1.a]: Electron Magnetic Moment vs $\left(\frac{T}{m}\right)^2$

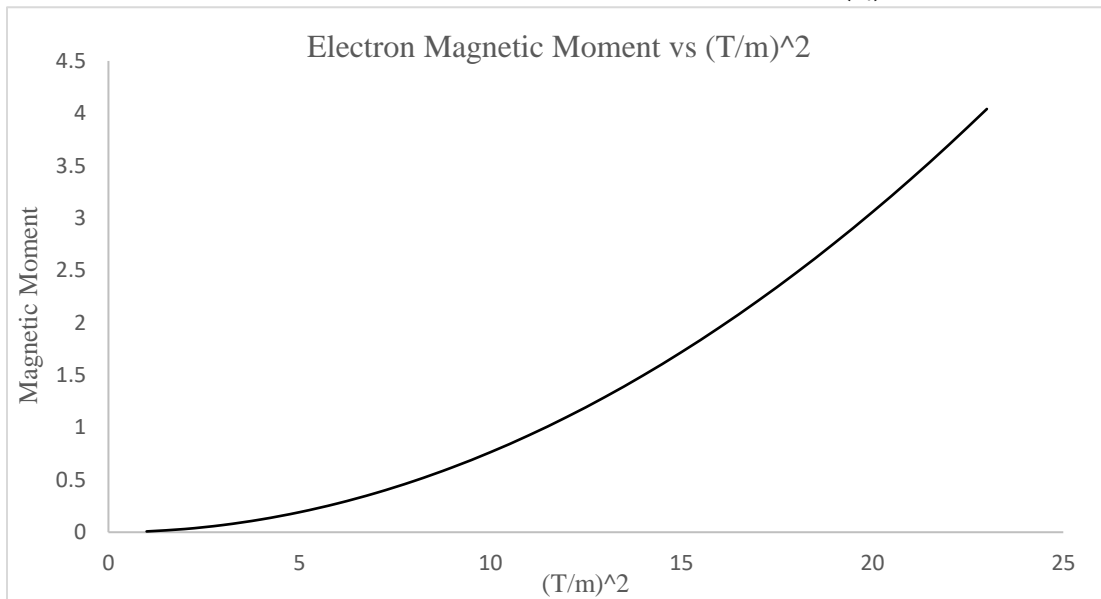


Figure [5.1.1.b]: Muon Magnetic Moment vs $\left(\frac{T}{m}\right)^2$

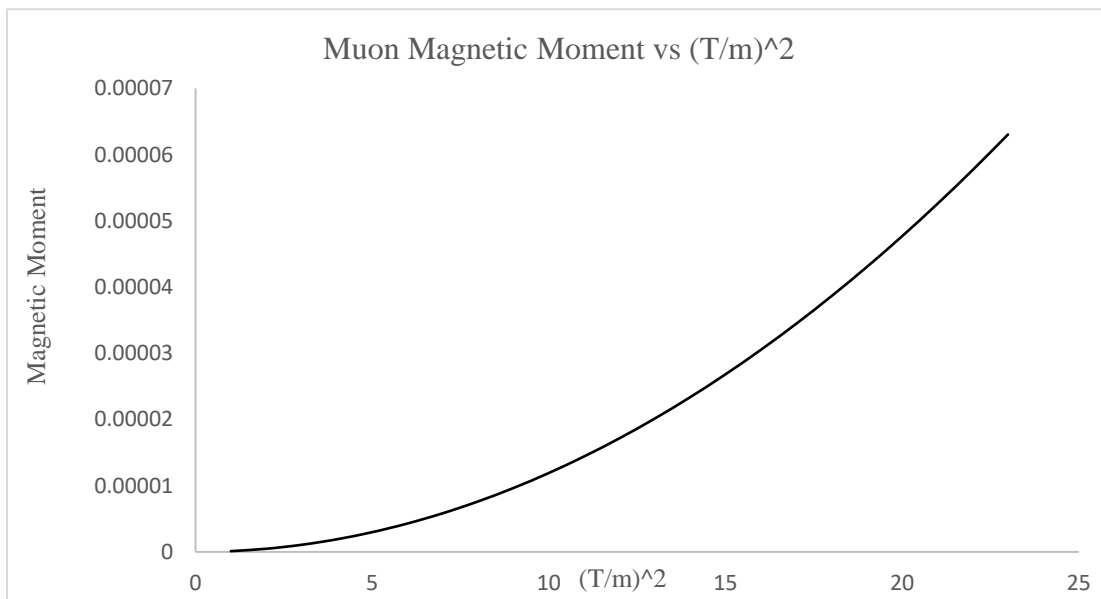


Figure [5.1.1.c]: Tau Magnetic Moment vs $\left(\frac{T}{m}\right)^2$

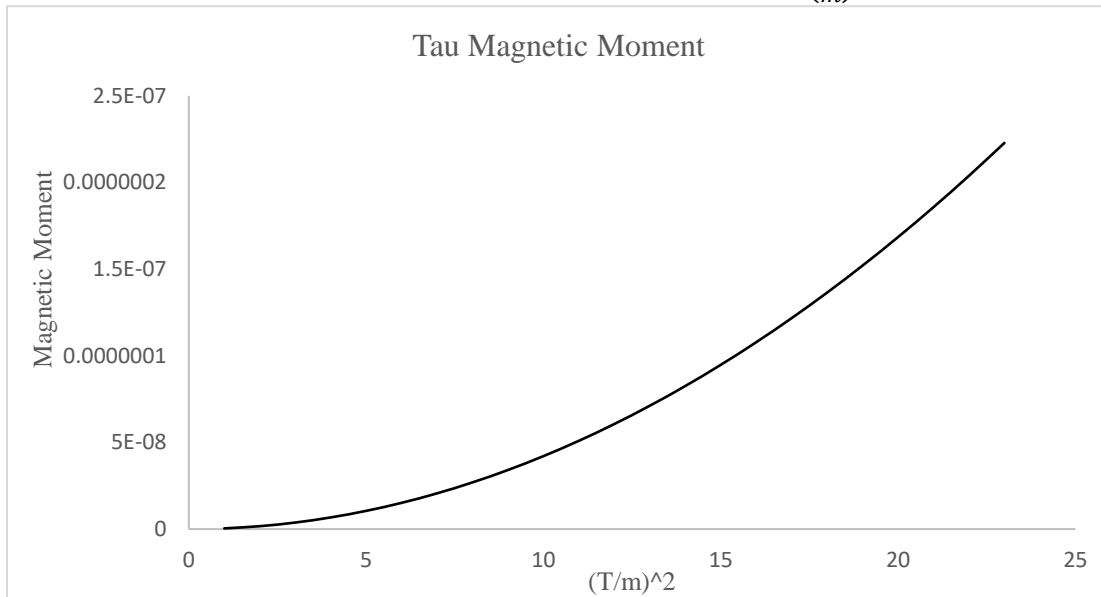
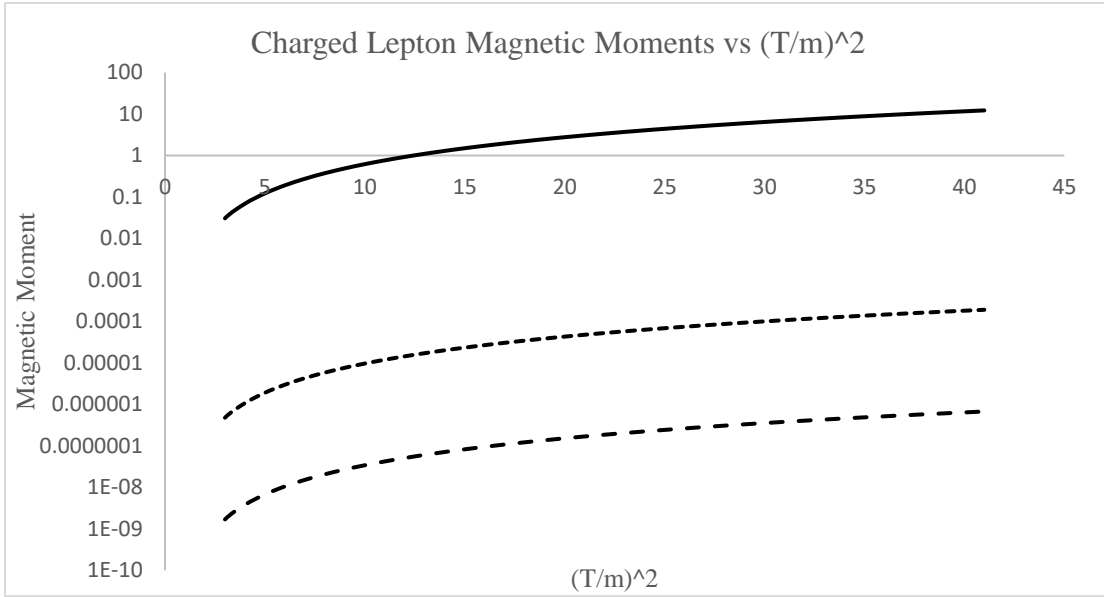


Figure [5.1.1.a] shows an interesting result that the magnetic moment flips as the temperature approaches 0.22 MeV. This flip will also occur for muons and tauons, but not until the temperatures reach a much larger value. This means that the contributions to the heavier charged particles are ignorable during nucleosynthesis.

Figures [5.1.1.b] and [5.1.1.c] show that the higher the temperature, the more important the contributions to magnetic moment are.

Figure [5.1.2] is a comparison of magnetic moment vs temperature for all three charged leptons. The solid line represents the electron, the dotted line represents the muon, and the dashed line represents the tau.

Figure [5.1.2]: Charged Lepton Magnetic Moment vs $\left(\frac{T}{m}\right)^2$



The thermal contributions to charged leptons near nucleosynthesis temperature ($T \sim m_e$) is calculated and presented in the following Table [5.1.1]. We did not include the contributions from the a,b,c coefficients because it does not change the order of magnitude.

Table [5.1.1]: Magnetic Moment of Charged Leptons around Nucleosynthesis in the Universe

Charged Leptons	Mass (eV)	Corresponding Temperature (K)	Magnetic Moment at T=0 (μ_B)	Thermal Contribution at T= m_e (μ_B)
e	0.511×10^6	0.592×10^{10}	1	-7.6×10^{-3}
μ	105.65×10^6	0.122×10^{13}	4.8×10^{-3}	-1.19×10^{-7}
τ	1776.82×10^6	0.206×10^{14}	2.8×10^{-4}	-4.2×10^{-11}

The neutrino masses for both the upper and lower mass bounds are both small values, but they are still nonzero and need to be calculated and understood.

The below figures show the relationship between the magnetic moment of the three different flavors of neutrinos and temperature. We are using the same temperature as the charged lepton for comparison purposes. The first set of four figures is for the upper bound masses that was calculated for the neutrino. The second set of figures is for the lower bound neutrino masses. Figure [5.1.3] shows how temperature effects all of the flavors. Plotting these three flavors of neutrinos, next to one another, shows the difference more clearly between the flavors' magnetic moments with increased temperature. The following figures plot each flavor of neutrino separately for a more detailed graph. These graphs all appear to be linear in lower temperature, but as the temperature increases, it becomes apparent that it is quadratic.

Figure [5.1.3]: Upper Bounds: Neutrino Magnetic Moment vs $\left(\frac{T}{m}\right)^2$

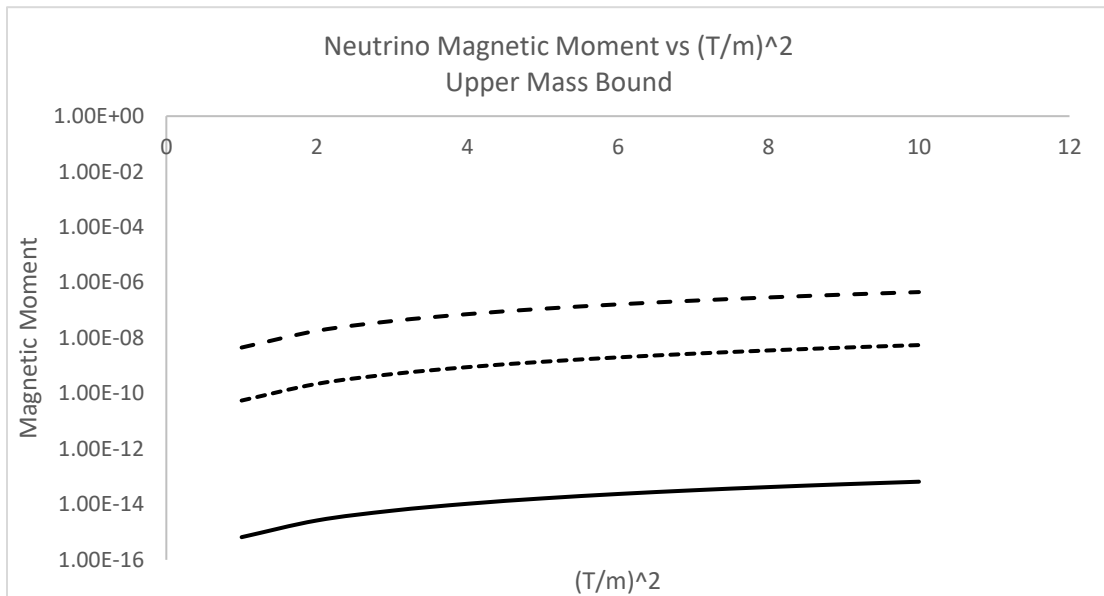


Figure [5.1.4.a]: Upper Bounds: Electron Neutrino Magnetic Moment vs $\left(\frac{T}{m}\right)^2$

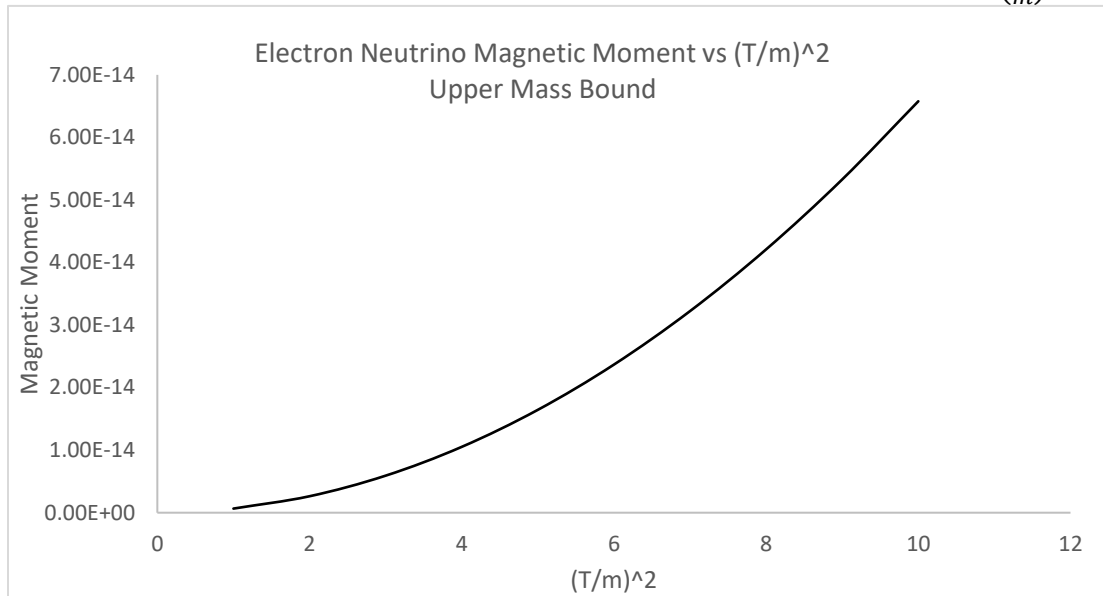


Figure [5.1.4.b]: Upper Bounds: Muon Neutrino Magnetic Moment vs $\left(\frac{T}{m}\right)^2$

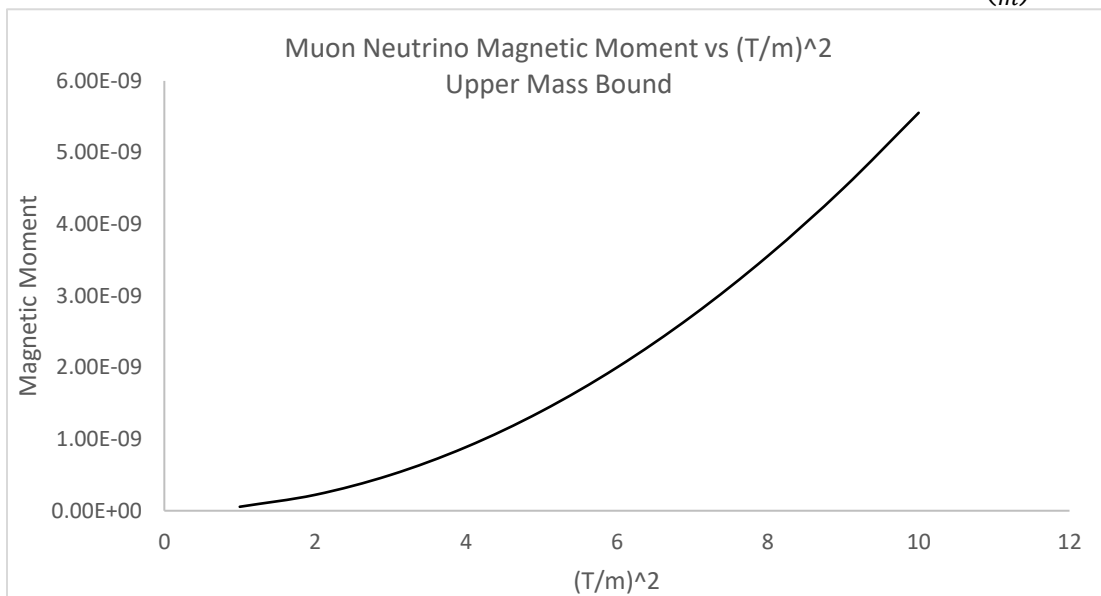
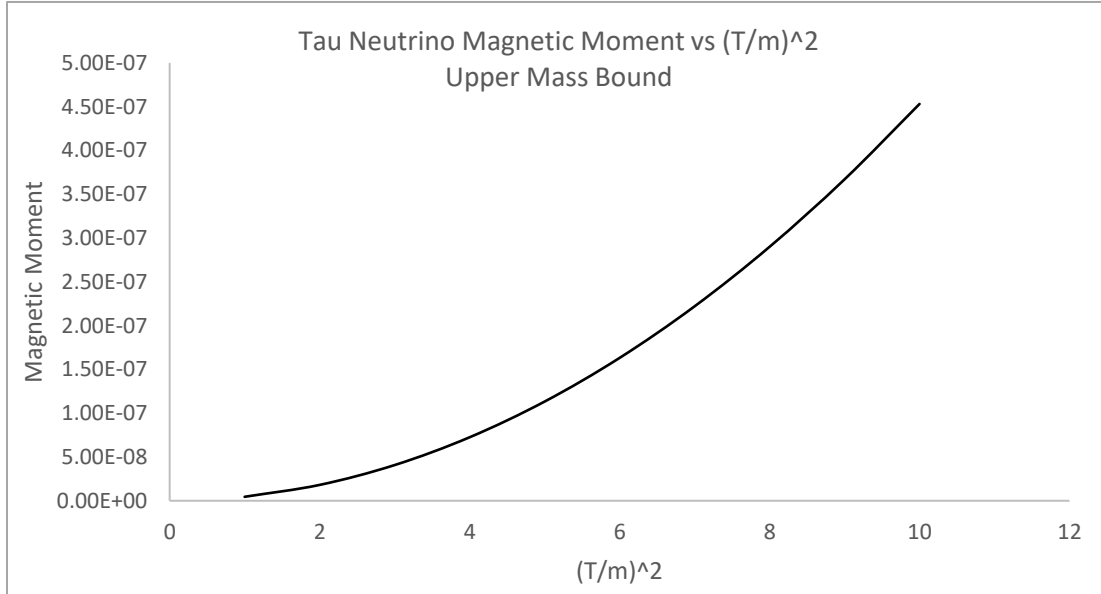


Figure [5.1.4.c]: Upper Bounds: Tau Neutrino Magnetic Moment vs $\left(\frac{T}{m}\right)^2$



The following tables for the upper and lower bounds of neutrino masses use the bubble diagrams from Chapter II. The tadpole diagrams do not contribute in the early universe because of CP symmetry. Tables [5.1.2.a] and [5.1.2.b] shows the proportional relationship between mass and magnetic moment. This shows why the tau neutrino has the largest magnetic moment because of its corresponding large mass. The tables also show the temperature contributions to the magnetic moment near nucleosynthesis temperatures that correspond to the neutrino masses. The results found in this thesis can be easily updated with newer experiments improved mass values.

Table [5.1.2.a]: Magnetic Moment of Neutrinos (Upper Bounds)

Neutrino Flavor	Mass (eV)	Corresponding Temperature (K)	Magnetic Moment at T=0 (μ_B)	Magnetic Moment with Thermal Contribution at T=me (μ_B)
ν_e	2.25	2.6×10^4	7.2×10^{-19}	6.58×10^{-16}
ν_μ	1.9×10^5	2.2×10^9	6.08×10^{-14}	5.55×10^{-11}
ν_τ	1.82×10^7	2.1×10^{11}	5.83×10^{-12}	4.53×10^{-9}

Table [5.1.2.b]: Magnetic Moment of Neutrinos (Lower Bounds)

Neutrino Flavor	Mass (eV)	Temperature (K)	Magnetic Moment at T=0 (μ_B)	Magnetic Moment with Thermal Contribution at T=me (μ_B)
ν_e	1.4×10^{-5}	0.162192	4.48×10^{-24}	4.12×10^{-21}
ν_μ	2.8×10^{-3}	32.48	8.96×10^{-22}	8.24×10^{-19}
ν_τ	4.8×10^{-2}	556.8	1.54×10^{-20}	1.41×10^{-17}

Figure [5.1.5]: Lower Bounds: Neutrino Magnetic Moment vs $\left(\frac{T}{m}\right)^2$

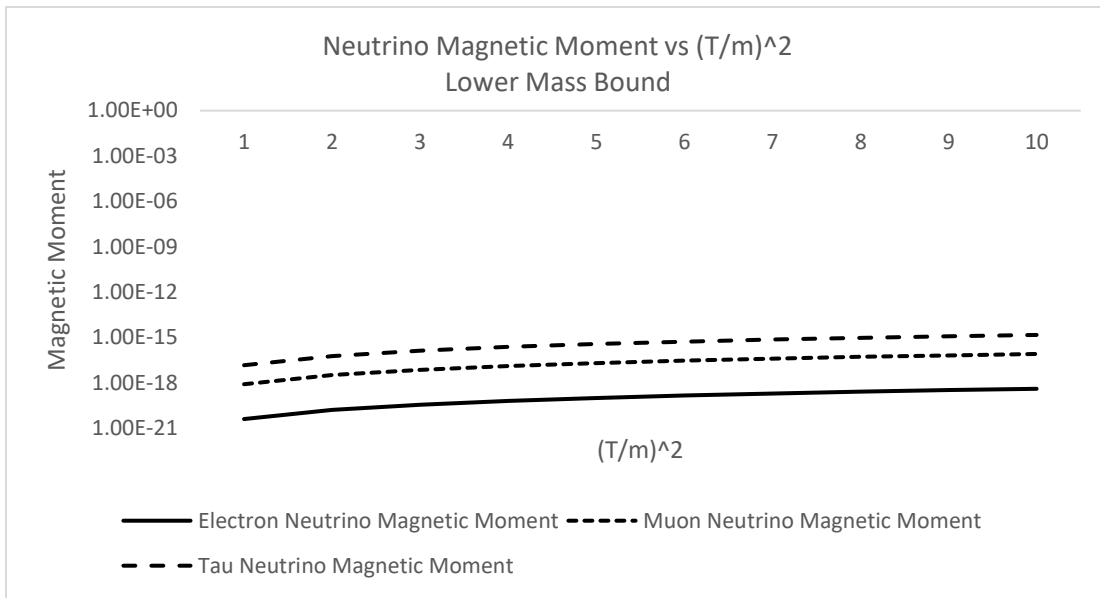


Figure [5.1.6.a]: Lower Bounds: Electron Neutrino Magnetic Moment vs $\left(\frac{T}{m}\right)^2$

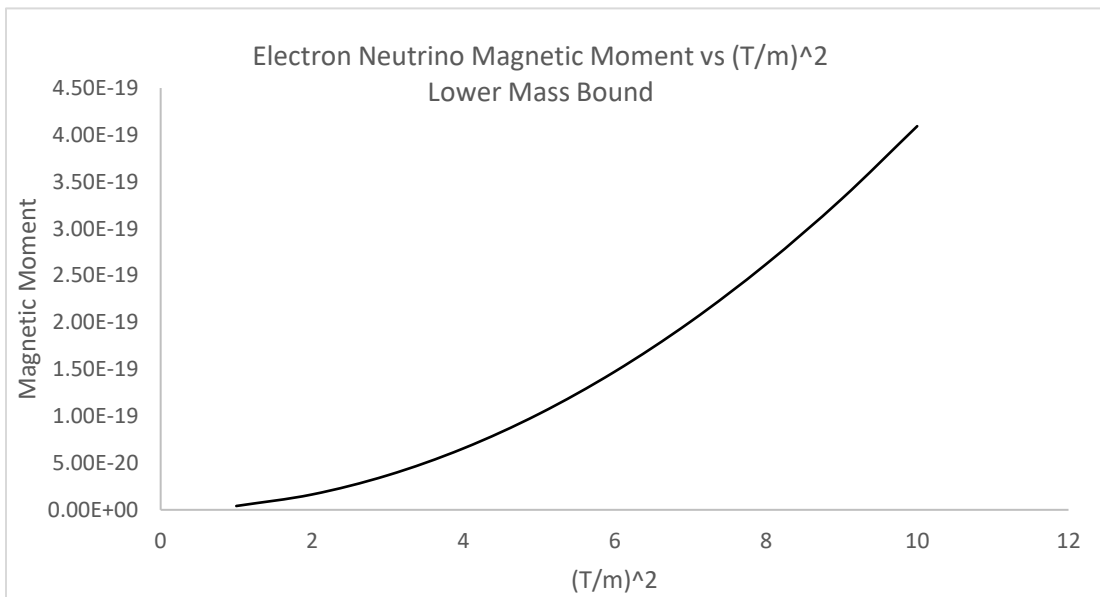


Figure [5.1.6.b]: Lower Bounds: Muon Neutrino Magnetic Moment vs $\left(\frac{T}{m}\right)^2$

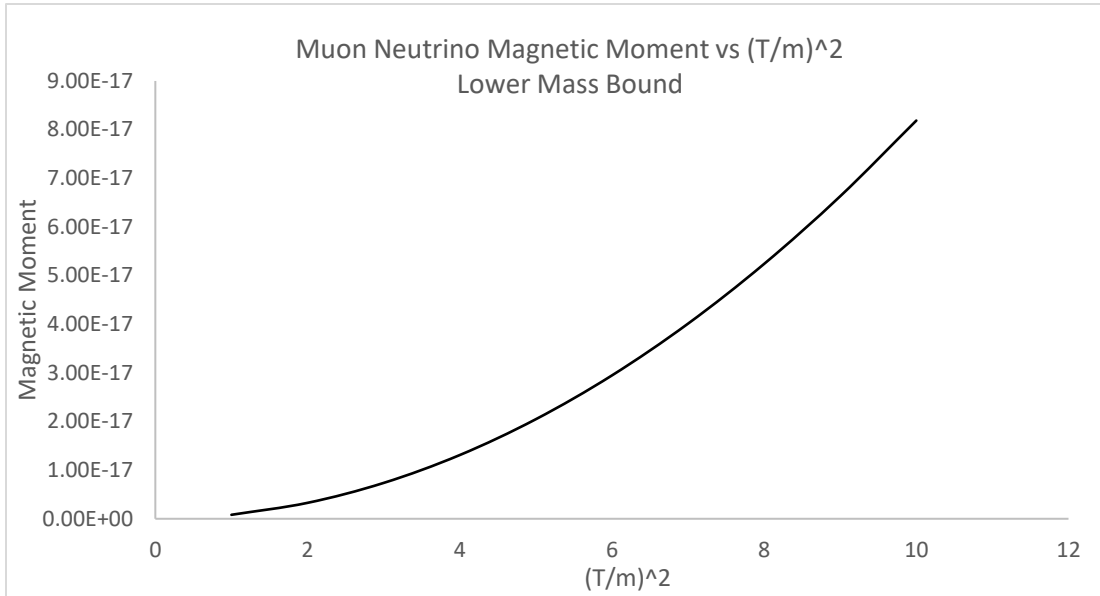
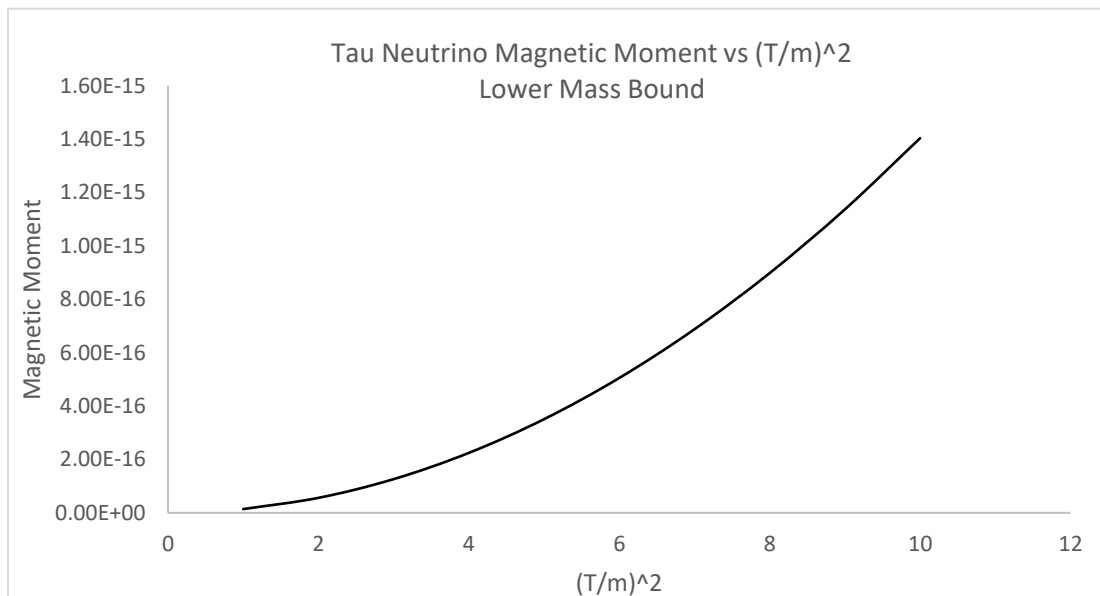


Figure [5.1.6.c]: Lower Bounds: Tau Neutrino Magnetic Moment vs $\left(\frac{T}{m}\right)^2$



In conclusion, we give the calculations of the magnetic moment of Dirac neutrinos, in the minimally extended standard model, near the nucleosynthesis temperatures to show that the magnetic moment of charged leptons and neutrinos pick up thermal corrections in different ways. Thermal corrections to charged leptons are inversely proportional to the mass of leptons; whereas thermal corrections to neutrinos are proportional to the corresponding lepton mass.

This work can be extended in different directions to include extensions of the standard model. The relevant applications in astrophysics and cosmology can also be discussed in more detail. However, in cosmology, temperature is the only statistical parameter; whereas in astrophysics, chemical potential can also be included. The magnetic field effect on some stellar objects, such as neutron stars, should be studied in detail as well.

REFERENCES

1. Ahmed, K.; Masood, S.S.: Renormalization and radiative corrections at finite temperature reexamined. *Phys. Rev. D* 35,1861 (1987)
2. Ahmed, K.; Masood, S.S.: Finite-temperature and-density renormalization effects in QED. *Phys. Rev. D* 35, 4020 (1987)
3. Ahmed, K.; Masood, S.S.: Vacuum polarization at finite temperature and density in QED. *Ann. Phys.* 164, 460 (1991)
4. Brogini, C., Giunti, C., & Studenikin, A. (2012). Electromagnetic properties of neutrinos. *Advances in High Energy Physics*, 2012.
5. Chaichian, M., Masood, S., Montonen, C., Aperez Martinez, and H.Perez Rojas 'Quantum Magnetic Collapse' *Phys. Rev. Lett.* 84 5261 (2000).
6. Couchot, F., Henrot-Versillé, S., Perdereau, O., Plaszczynski, S., d'Orfeuil, B. R., Spinelli, M., & Tristram, M. (2017). Cosmological constraints on the neutrino mass including systematic uncertainties. *Astronomy & Astrophysics*, 606, A104.
7. Czarnecki, A., & Marciano, W. J. (2001). Muon anomalous magnetic moment: A harbinger for "new physics". *Physical Review D*, 64(1), 013014.
8. Davidson, S., Hannestad, S., & Raffelt, G. (2000). Updated bounds on milli-charged particles. *Journal of High Energy Physics*, 2000(05), 003.
9. Eidelman, S., & Passera, M. (2007). Theory of the τ lepton anomalous magnetic moment. *Modern Physics Letters A*, 22(03), 159-179.
10. Elmfors, P., Grasso, D., & Raffelt, G. (1996). Neutrino dispersion in magnetized media and spin oscillations in the early universe. *arXiv preprint hep-ph/9605250*.
11. Fornengo, N., Kim, C. W., & Song, J. (1997). Finite temperature effects on the neutrino decoupling in the early universe. *Physical Review D*, 56(8), 5123.
12. Fujikawa, K., & Shrock, R. E. (1980). Magnetic moment of a massive neutrino and neutrino-spin rotation. *Physical Review Letters*, 45(12), 963.
13. Griffiths, D. (2008). *Introduction to elementary particles*. John Wiley & Sons.
14. Haseeb, M.; Masood, S.S.: Second order thermal corrections to electron wavefunction. *Phys. Lett. B* 704, 66 (2011)
15. Kinoshita, T.: Mass singularities of Feynman amplitudes. *J. Math. Phys.* **3**, 650 (1962)
16. Kobes, R.: A correspondence between imaginary time and real time finite temperature field theory. *Phys. Rev. D* 42, 562 (1990).
17. Kumericki, K. (2016). Feynman diagrams for beginners. arXiv preprint arXiv:1602.04182.
18. Landsman, P. and Weert, Real-and imaginary-time field theory at finite temperature and density. *Phys. Rep.* 145, 141 (1987)

19. Lee, B.W. and Shrock, R.E. (1977) Natural Suppression of Symmetry Violation in Gauge Theories: Muon-and Electron-Lepton-Number Nonconservation. *Physical Review D*, **16**, 1444. <http://dx.doi.org/10.1103/PhysRevD.16.1444>
20. Ma, E., & Raidal, M. (2001). Neutrino mass, muon anomalous magnetic moment, and lepton flavor nonconservation. *Physical Review Letters*, *87*(1), 011802.
21. Masood, Samina and Haseeb, Mahnaz, 'Two loop temperature corrections to electron self-energy', *Chin. Phys. C* *35*, 608 (2011).
22. Masood, S.S.: Finite-temperature and-density effects on electron self-mass and primordial nucleosynthesis. *Phys. Rev. D* *36*, 2602 (1987)
23. Masood, S.S.: Photon mass in the classical limit of finite-temperature and-density QED. *Phys. Rev. D* *44*, 3943 (1991)
24. Masood, S.S.; Haseeb, M.Q.: Gluon polarization at finite temperature and density. *Astropart. Phys.* *3*, 405 (1995)
25. Masood, S.: Renormalization of QED near decoupling temperature. *Phys. Res. Int.* *2014*, 48913 (2014). arXiv:1407.1414
26. Masood, S.S.: Nucleosynthesis in hot and dense media. *JMP* *5*, 296 (2014). <https://doi.org/10.4236/jmp.2014.55040>
27. Masood, Samina, 'QED Plasma in the Early Universe', *Arabian Journal of Mathematics* (2019).
28. Masood, S.S.: Propagation of monochromatic light in a hot and dense medium. *Euro. Phys. J.C* *77*, 826 (2017). <https://doi.org/10.1140/epjc/s10052-017-5398-0>.
29. Masood, S. S. (2018). QED Plasma at Finite Temperature up to Two Loops. arXiv preprint arXiv:1808.10769.
30. Masood, S. S. (1993). Neutrino physics in hot and dense media. *Physical Review D*, *48*(7), 3250.
31. Masood, S. S. (2015). Magnetic Dipole Moment of Neutrino. *arXiv preprint arXiv:1506.01284*.
32. Masood, Samina, A. Perez Martinez, H. Perez Rojas, R. Gaitan, and S. Rodriguez Romo 'Effective Magnetic Moment of Neutrinos in the Strong Magnetic Fields', *Rev.Mex.Fis.* *48*, 501 (2002).
33. Masood, Samina, 'Magnetic Moment of Neutrino in the Statistical Background', *Astroparticle Phys.* *4*, 189 (1995).
34. Masood, Samina and Haseeb, Mahnaz, 'Second Order Corrections to Magnetic Moment of Electron at Finite Temperature', *IJMPA*, *A27*, 1250188 (2012).
35. Nieves, J.F.; Pal, P.B.: P- and CP-odd terms in the photon self-energy within a medium. *Phys. Rev. D* *39*(2), 652 (1989).
36. Nowakowski, M., Paschos, E. A., & Rodriguez, J. M. (2005). All electromagnetic form factors. *European journal of physics*, *26*(4), 545.

37. Pal, P. B., Particle physics confronts the solar neutrino problem, *Int.J.Mod.Phys. A7* (1992) 5387–5460.
38. Peltoniemi, J., & Sarkamo, J. (1997). Laboratory measurements and limits for neutrino properties.
39. Peltoniemi, J. T., & Valle, J. W. (1993). Reconciling dark matter, solar and atmospheric neutrinos. *Nuclear Physics B*, 406(1-2), 409-422.
40. Perkins, D. H. (2000). *Introduction to high energy physics*. Cambridge University Press.
41. Riotto, A. (1994). Thermal background corrections to the neutrino electromagnetic vertex in models with charged scalar bosons. *Physical Review D*, 50(3), 2139.
42. Roberts, B. L., & Marciano, W. J. (2010). *Lepton dipole moments (Vol. 20)*. World Scientific.
43. Studenikin, A. I. (2016). Electromagnetic neutrino: a short review. *Nuclear and particle physics proceedings*, 273, 1711-1718.
44. Tanabashi, Masaharu, et al. "Review of particle physics." *Physical Review D* 98.3 (2018): 030001.